CHAPTER FIVE

CALC-SILICATES REACTION BANDS

5.1 INTRODUCTION

Many examples of calc-silicate reaction bands occur in the impure calcirudites described in Chapter Four. They consist of chemically distinct mineral layers (or zones) separating orginally adjacent chemically incompatible lithologies within the calcirudite. Calc-silicate reaction bands (also termed diffusion zones, diffusion skarns, and metamorphic skarns, by various authors) have been investigated by several workers, including Vidale (1969), Brock (1972), Hewitt (1973), Vidale and Hewitt (1973), Joesten (1974,1977) Thompson (1975a), Brady (1977), Kerrick (1977), Sanford (1980) and Hoersch (1981), all of whom assign their formation to the diffusion of components through a pore solution in response to chemical potential gradients.

The aim of this chapter is to petrologically examine several small-scale examples of these reaction bands, in an attempt to delineate the relative movement of components across the layers. Detailed thin-section descriptions, modal analyses (by point counting), and probe analyses of all phases involved have been undertaken to achieve this aim. In discussing the formation of the calc-silicate reaction bands it has been convenient (in line with recent studies) to make use of the concepts of local equilibrium, chemical potential gradients, and J and K components distinguished by the internal or external control of their chemical potentials (Thompson, 1970). These concepts are outlined in Section 5.9.1.

This work involves only a qualitative study of the movement of elements relative to each other and the initial contact. No attempt is made to quantitatively determine rates of diffusion, nor to describe the chemical processes occurring during diffusion.

5.2 LOCATION AND FIELD DESCRIPTION

The calc-silicate reaction bands studied in most detail were sampled from a costean that cuts across the western limestone horizon of the Horse

Arm Creek locality, north of the Inlet Monzonite (Fig. 5-1). This limestone unit has been described in Chapter Four. The costean is sited approximately 350m from the contact of the Inlet Monzonite. At this costean, the impure calcirudites consist of large rounded blocks of marble and angular blocks (commonly elongate lenses) of fine-grained biotite-rich metasediment, within a matrix dominated by garnet (Plate 5-1A). The marble blocks are most abundant, ranging in size from small nodules (1-2 cm) up to boulders over 20 cm in diameter. They are composed almost entirely of medium- to coarse-grained calcite, but the grey-white colour of the marble is typically spotted with coarse brown garnets. In contrast, the biotite-rich blocks are exceptionally fine grained, and have a characteristic black colour. The garnet-rich matrix surrounds these individual blocks, and although the matrix can occupy up to 50% of the rock, in some samples it is only a relatively minor component. The garnet grains within this matrix are generally between 1-2 mm in diameter, euhedral in shape, and have a characteristic brown colour. Irregularly shaped patches of calcite and copper sulphides (chalcopyrite and bornite can be recognised in hand specimen) commonly occur amongst the garnet-rich matrix.

In hand specimen, layers within the reaction bands, occurring between the chemically distinct parts of these rocks, are well outlined by sharp changes in colour (further layers have been elucidated by detailed thin-section observation, Section 5.4). Where the matrix is in contact with blocks of marble, wollastonite-rich rims (up to 2-3 cm wide) occur within the outlines of the original marble (Plate 5-1B). The wollastonite is bladed and has a cream-white colour. These rims can consist of pure wollastonite, though commonly they are a mixture of wollastonite, garnet and small patches of copper sulphides. Where the garnet-rich matrix contacts the dark biotite-rich metasediment, the margin of the metasediment is replaced by fine-grained green rims of clinopyroxene. If replacment of this type is particularly extensive, a grey to grey-green layer can also be recognised in hand specimen between the distinctly green layer and the black sediment (Plate 5-1C). This layer is variable in its occurrence, for although it is often missing, it can be quite wide, sometimes to the exclusion of the green clinopyroxene layer. Contacts between the blocks of marble and biotite-rich metasediment are not common. Interestingly, where such contacts do occur, the resultant reaction band

Figure 5-1: Location of the costean (sample locality 371) from which the major examples of calc-silicate reaction bands were sampled. Other samples described in Sections 5.10 and 11 are also shown.

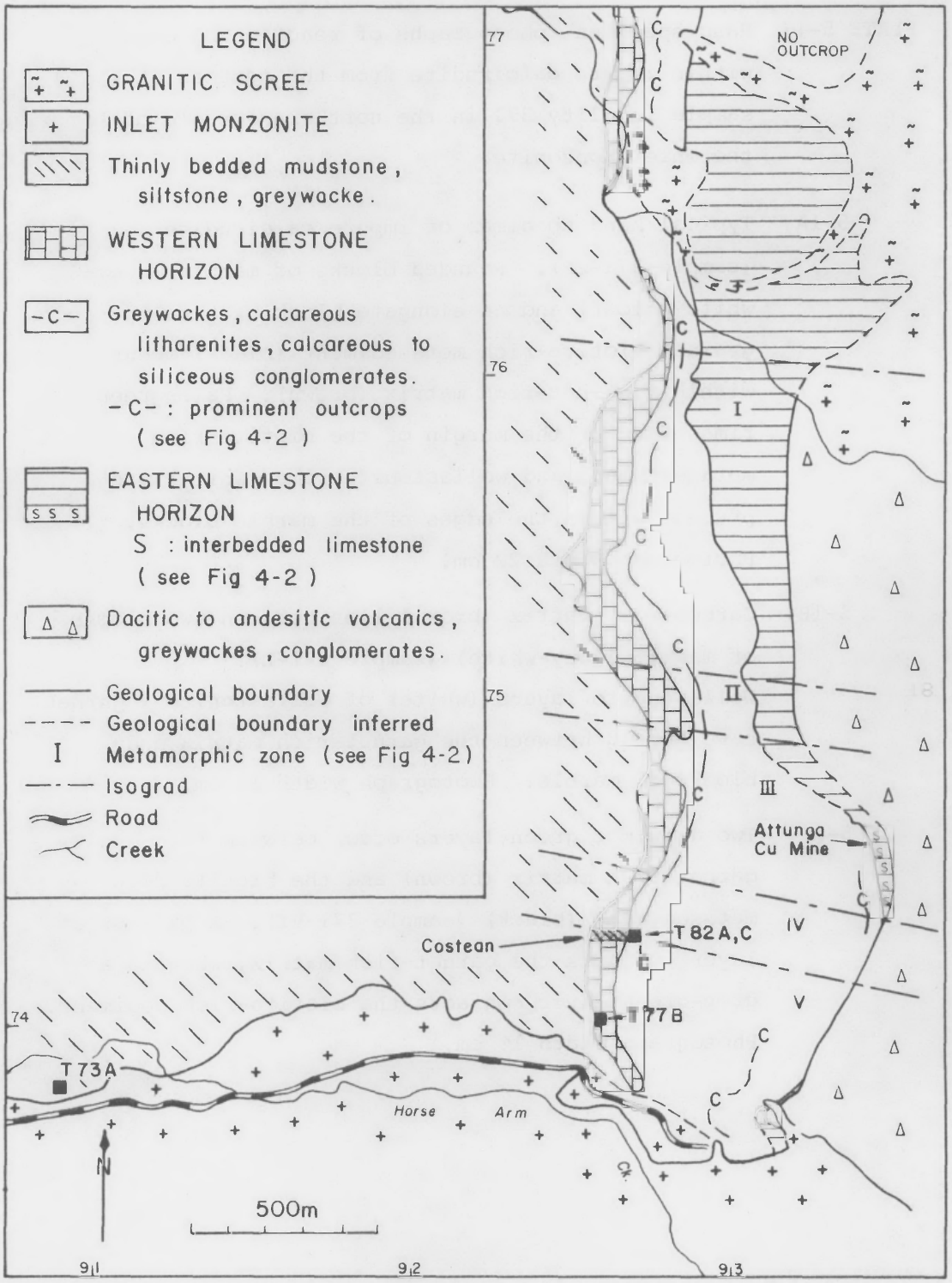
LEGEND
GRANITIC SCREE
INLET MONZONITE
Thinly bedded mudstone, siltstone, greywacke.
WESTERN LIMESTONE HORIZON
-C-
Greywackes, calcareous litharenites, calcareous to siliceous conglomerates.
-C- : prominent outcrops (see Fig 4-2)
EASTERN LIMESTONE HORIZON
S S S
S : interbedded limestone (see Fig 4-2)
Dacitic to andesitic volcanics, greywackes, conglomerates.
Geological boundary
Geological boundary inferred
I Metamorphic zone (see Fig 4-2)
Isograd
Road
Creek
NO OUTCROP
Attunga Cu Mine
Costean
T82A,C
T77B
T73A
Horse
Arm
N
500m
77
76
75
74
91
92
93

PLATE 5-1: Hand specimen photographs of reaction bands within impure calcirudite from the costean at sample locality 371 in the northern aureole of the Inlet Monzonite.

5-1A: Typical hand specimen of impure calcirudite (sample 371-PB). Rounded blocks of marble (grey-white colour) and an elongate block of fine-grained biotite-rich metasediment (black) occur within a garnet-rich matrix (brown). Pale-green rims exist at the margin of the biotite-rich metasediment, and wollastonite rims (white) are present within the edges of the marble blocks. Photograph width 22 cm.

5-1B: Garnet-rich matrix (brown) lies between two blocks of marble (grey-white) (sample 371-L). Wollastonite layers (white) of wollastonite + garnet have formed between the garnet-rich matrix and blocks of marble. Photograph width 14 cm.

5-1C: Two distinct green layers occur between the garnet-rich matrix (brown) and the biotite-rich metasediment (black) (sample 371-VI). A pale-green layer contacts the garnet-rich matrix, whereas a grey-green layer contacts the biotite-rich sediment. Photograph width 10 cm.

A

B

C

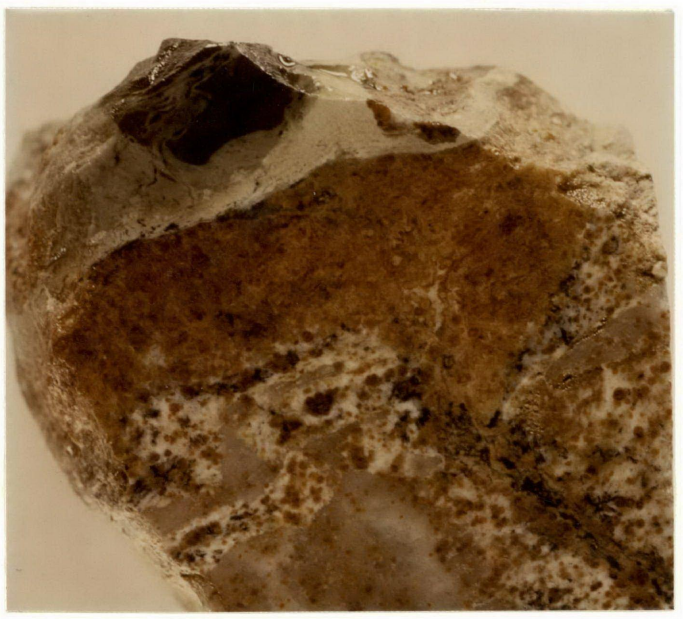

is typically very thin (usually only a couple of mm). Even so, distinct layers of brown garnet and green clinopyroxene can always be distinguished (Plates 5-2A and B). Notably, however, a wollastonite layer does not occur. The thinness of these layers and their characteristic lack of wollastonite are dealt with in later sections.

Although detailed study of samples from the costean (sample locality 371) comprise the major part of this study, numerous other examples of reaction bands from the Horse Arm Creek and South Kootingal localities (Chapter Four, Figs. 4-1A and B) were petrographically and chemically investigated. Two examples of these are briefly discussed at the end of this chapter. Finally, large-scale diffusion has been recognised at the Horse Arm Creek locality between the western limestone unit and the underlying greywackes. The greywackes adjacent to the limestone, although texturally identical to those further away, have a distinctly greener colour, characteristic of the presence of clinopyroxene. Thin-section studies, probe analyses, and whole-rock analyses were made on both the "unaffected" greywacke (T82C) and that adjacent to the limestone (T82A). These samples are located in Fig. 5-1.

5.3 P-T CONDITIONS

Metamorphic conditions have been estimated in Chapter Four for the Horse Arm Creek locality, using the calcareous litharenites. Pressures below 2 kb have been estimated within the aureole. The costean (sample locality 371) from which the major samples of this chapter have been collected occurs, as noted above, approximately 350m from the contact. This distance broadly marks the beginning of the wollastonite + plagioclase zone, where wollastonite is stable in textural equilibrium with plagioclase An 30. Temperatures for this boundary have been estimated at between 610^{o} and 650^{o}C depending on the actual pressure of metamorphism (Figs. 4-7 and 4-8).

5.4 PETROGRAPHY

5.4.1 Introduction

The petrography characteristic of several well delineated reaction

PLATE 5-2: Hand specimen photographs of reaction bands in sample 371-1 from the northern aureole of the Inlet Monzonite.

5-2A: A thin reaction band is present between blocks of marble (grey-white) and biotite-rich metasediment (black) (top left of photograph, enlargement shown in Plate 5-2B). However, the garnet-rich matrix (brown) separates the various blocks in most of the sample. Wollastonite rims (white) are evident at the edges of marble blocks in contact with the garnet-rich matrix. Photograph width 16.5 cm.

5-2B: An enlargement of the reaction band between marble and biotite-rich metasediment in Plate 5-2A (centre top). Thin layers of green clinopyroxene and brown garnet occur between the two blocks. The reaction band between the marble and biotite-rich metasediment is much thinner than between garnet-rich matrix and the biotite-rich metasediment. Wollastonite is prominent between the garnet-rich matrix and marble, but is absent between marble and biotite-rich metasediment. Photograph width 7.5 cm.

A

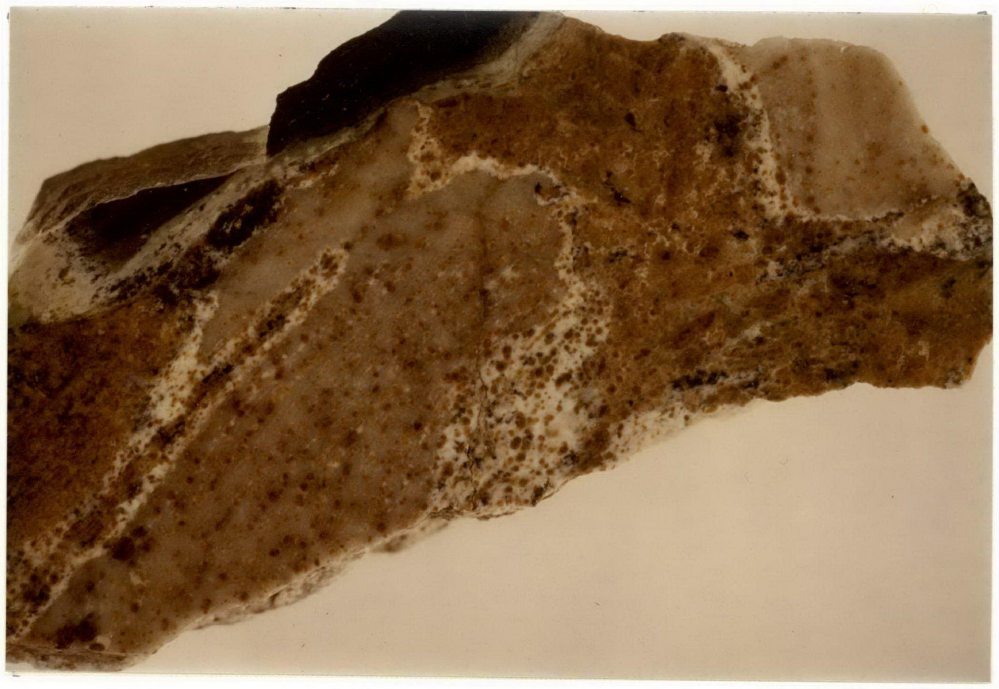

B

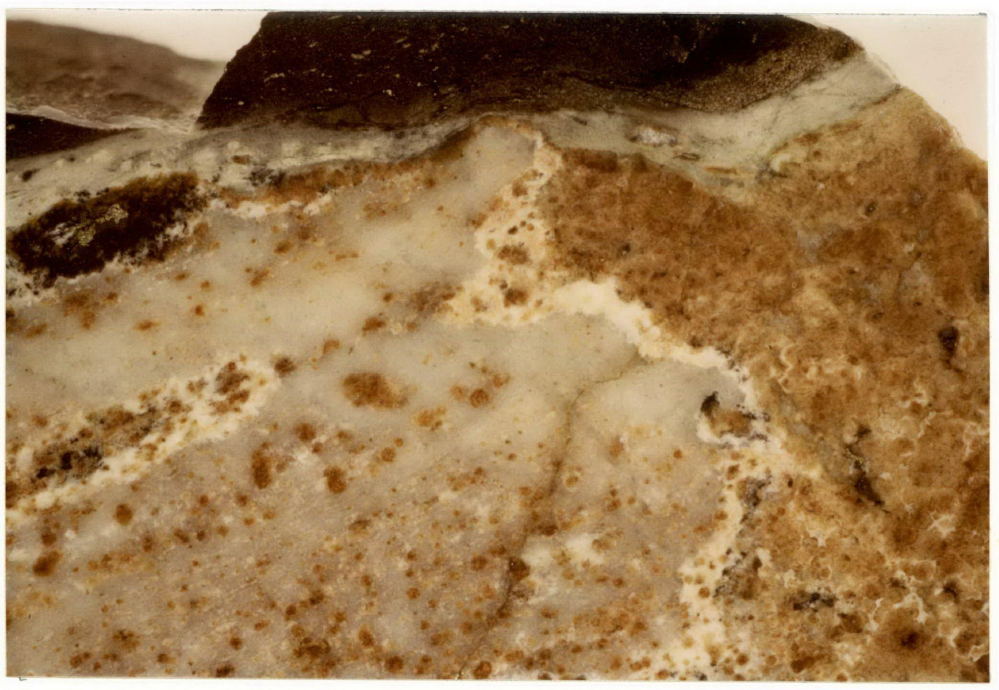

bands from sample locality 371 is described in this section. Their description is typical of reaction bands throughout the costean. Layering within the reaction bands of these rocks are of three types:

1) layers produced between orginally contacting blocks of marble and biotite-rich metasediment;

2) layers produced between garnet-rich matrix and biotite-rich metasediment;

3) layers produced between garnet-rich matrix and marble.

The biotite-rich metasediment now consists mainly of biotite, K-feldspar and plagioclase. It is perhaps inappropriate to refer to this assemblage as pelitic, and in this description it is simply referred to as the biotite + feldspar unit. Thompson (1975a), in his description of a reaction band between marble and pelite, observed no muscovite or Al-silicate in the pelite next to the calc-silicate zones, and suggested that their absence may be related to the diffusion. Similarly, evidence is presented later in this chapter to suggest that the biotite + feldspar unit does not accurately represent the original non-carbonate material within these rocks, but is pelite that has been slightly chemically modified by Ca diffusion during formation of the reaction bands. Therefore, pelite is assumed to have been the original non-carbonate material involved in the formation of the reaction bands.

Modal analyses (from point counting) and widths of the layers within the traverses studied in this section are given in Table 5.1. The mineralogy is typically homogeneous within the layers, and point counts were taken from as large an area as possible within each layer. The accuracy of some of the modes is limited by the very fine grainsize.

5.4.2 Marble → Pelite Reaction Bands

The sequence of layers in this type of reaction band is:

marble
garnet
garnet + clinopyroxene
felsic (K-feldspar + sphene ± clinopyroxene ± plagioclase)
clinopyroxene + feldspar + sphene
biotite + feldspar + sphene
biotite + feldspar unit

TABLE 5.1. Modal analyses of selected traverses across reaction bands from sample locality 371

	Layer Width (mm)	Biotite	K-feldspar	Plagioclase	Sphene	Clino-pyroxene	Garnet	Wollastonite	Calcite	(Cu-Fe Sulphides)	Accessories
371-1A											
BI+FELD		49.84	14.56	35.60						(7.59)	{M-4.49 T-1.12}
BI+FELD+SPH	1.10	34.18	26.55	33.29	5.98					(1.68)	
CPX+FELD+SPH	0.60		21.11	33.44	7.95	37.50				(3.30)	
FELSIC	0.18		65.47		9.60	24.93				(5.04)	
GT+CPX	0.15					77.97	22.03			(3.28)	
GT	0.35						100.00				
MARBLE						2.62	5.97		91.42		
371-VS2											
CPX+FELD+SPH			58.53	9.27	6.35	25.86					
FELSIC	0.25		56.51	17.96	6.93	18.60					
GT+CPX+K-F	0.25		26.67			26.67	46.66				
GT+CPX	0.65					56.85	43.15				
GT	0.93						100.00				
MARBLE									100.00		
371-1B											
BI+FELD		49.84	14.56	35.60						(7.59)	{M-4.49 T-1.12}
BI+FELD+SPH	1.90	34.18	26.55	33.29	5.98					(1.68)	
CPX+FELD+SPH	2.15										
CPX+FELD+SPH**	1.85		24.66	39.06	5.59	30.68				(0.65)	
FELSIC	0.25		72.62		†	27.38					
GT+CPX	0.22					62.82	37.18				
GT MATRIX						16.83	83.17		*(15.89)	(0.01)	
371-VI											
BI+FELD+SPH		23.16	22.98	46.20	7.66					(2.08)	
CPX+FELD+SPH	5.00		19.20	47.26	8.58	24.98				(0.77)	
CPX+FELD+SPH**	4.50		63.22		9.34	27.44				(1.18)	
FELSIC	0.38		55.31	28.62	†0.77	13.01					
GT+CPX	0.35					64.39	35.61				
GT MATRIX						13.53	86.47		*(5.74)		
371-L											
GT MATRIX						16.48	83.52		*(5.68)	*(0.04)	*{Q-7.32 P-0.29}
WOLL	16.00					7.32	42.32	50.36	*(6.82)		
MARBLE						4.35	18.81		76.84		

The values in brackets refer to phases occurring either in sulphide-rich veins or as secondary phases amongst the high-grade assemblage (* designates the latter). These phases are not considered as part of the general layer assemblage. Therefore, they are given as percentages of the total analysis, but are ignored in normalising the layer assemblage to 100%.

† Denotes that sphene is concentrated in a very thin rim between the felsic and garnet + clinopyroxene layers.
** Feldspar-altered part of the clinopyroxene + feldspar + sphene layer (see text).

Reaction band abbreviations: BI+FELD = biotite + feldspar unit, BI+FELD+SPH = biotite + feldspar + sphene layer, CPX+FELD+SPH = clinopyroxene + feldspar + sphene layer, FELSIC = felsic layer, GT+CPX+K-F = garnet + clinopyroxene + K-feldspar layer, GT+CPX = garnet + clinopyroxene layer, GT = garnet layer, WOLL = wollastonite layer, GT MATRIX = garnet-rich matrix.
Abbreviations for accessory phases: M = muscovite, T = tourmaline, Q = quartz, P = prehnite.

Two traverses (studies across a given reaction band) considered here show this type of layering. Traverse 371-1A shows the complete sequence, whereas 371-VS2 contains only part of it. This description will refer mainly to traverse 371-1A, for which the sequence of layering is shown in Plates 5-3A,B and C.

Marble

The marble blocks consist predominantly of medium-grained calcite showing excellent granoblastic-polygonal texture. The marble in 371-VS2 consists solely of calcite. However, in 371-1A it contains minor amounts of fine-grained equigranular clinopyroxene and coarse-grained garnets, typically along the calcite grain boundaries.

Garnet Layer

This is a monominerallic layer in which individual grains of garnet are difficult to distinguish. The garnet is characteristically colourless (or very pale brown) and has a distinct grey-blue anomalous interference colour.

Garnet + Clinopyroxene Layer

Garnet grains appear to be quite continuous from the garnet layer into the garnet + clinopyroxene layer. However, the boundary is sharply delineated by the presence of fine-grained equigranular clinopyroxene within the coarser-grained garnet (Plates 5-3A,B and C). The amount of clinopyroxene in this layer is variable, but it is consistently more abundant than the garnet (Table 5.1).

Felsic Layer

The felsic layer marks a significant change in texture and mineralogy compared to the previous layers. There is a major decrease in grainsize, which becomes similar to that in the biotite + feldspar unit (Plates 5-3A, B and C). The felsic layer also represents the first appearance of a K-containing phase (K-feldspar) and a Ti-containing phase (sphene). Though characteristic of the reaction bands, this layer is typically ill defined. It is usually very thin, and variable in modal composition. It consists mainly of K-feldspar + clinopyroxene + sphene, with K-feldspar dominant (Table 5.1, 371-1A). However, as shown by traverse 371-VS2 (Table 5.1), it may contain a significant amount of plagioclase (though this plagioclase

PLATE 5-3: Photomicrographs of the layer sequence across the marble → pelite reaction band in sample 371-1 (i.e. traverse 371-1A).

5-3A: Sequence of layers from marble to the biotite + feldspar + sphene layer (crossed polars). The slightly curved layers are delineated at the top and bottom of the photograph. M = marble, G = garnet layer, G-C = garnet + clinopyroxene layer, F = felsic layer, C-F-S = clinopyroxene + feldspar + sphene layer, B-F-S = biotite + feldspar + sphene layer (only the edge of this layer is shown). The layers are described in detail in the text. Only the broad features can be distinguished in this photograph.
Photograph width 3.60 mm.

5-3B and C: Identical enlargments across the felsic layer of the top part of the reaction band shown in Plate 5-3A, with Plate 5-3B taken under crossed polars and Plate 5-3C under plane-polarised light. The layers are labelled between the two photographs and abbreviations are the same as above. The width of both photographs is 0.90 mm.

The sharp boundary between the garnet + clinopyroxene and felsic layers, believed to be the original boundary between marble and pelite, is best shown in Plate 5-3C. Sphene is black in this photograph and is clearly concentrated in the felsic layer next to the garnet + clinopyroxene layer. The remainder of the felsic layer is dominated by K-feldspar. Alignment of sphene is quite distinct in the clinopyroxene + feldspar + sphene layer.

A

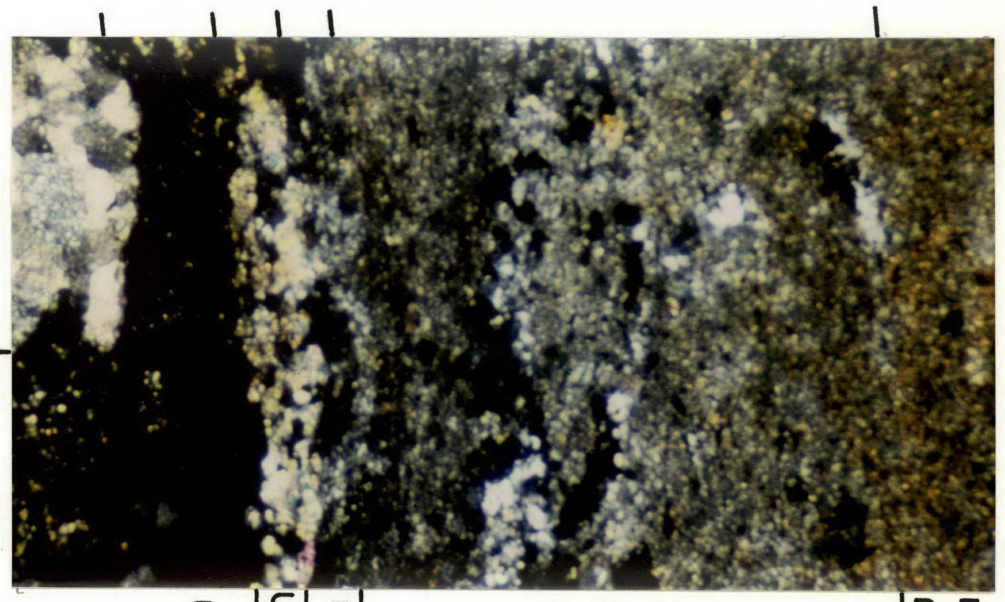

B

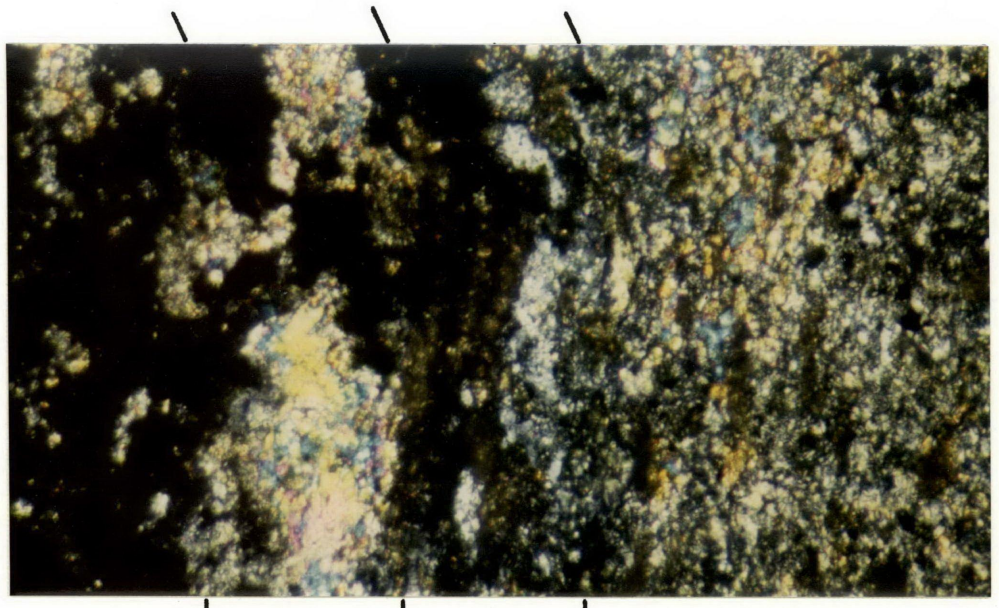

C

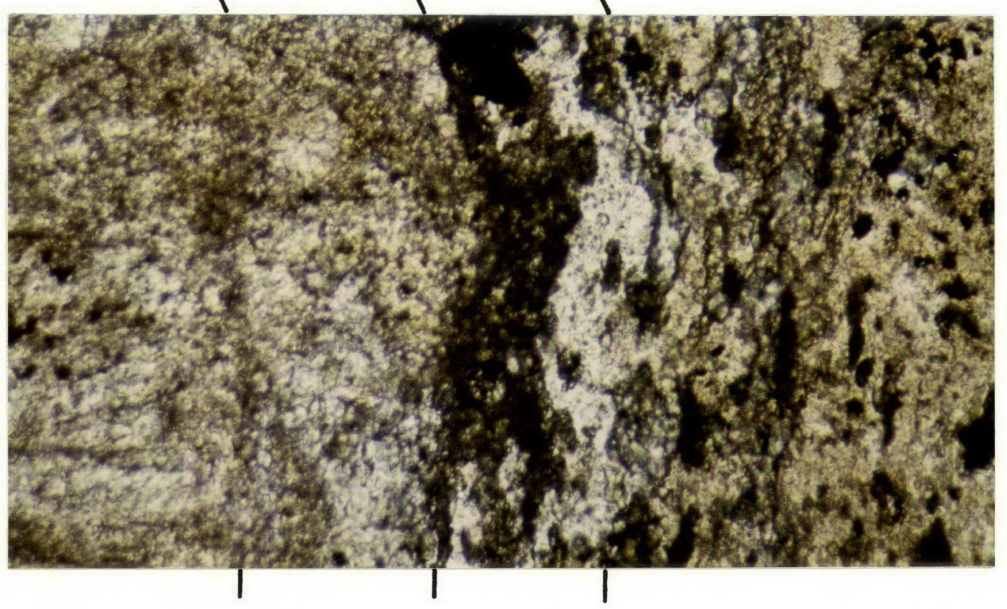

could be part of the adjacent clinopyroxene + feldspar + sphene layer). A very fine-grained brown aggregate of K-feldspar + sphene is characteristic of the felsic layer at its boundary with the clinopyroxene + garnet layer. Indeed, in some samples this K-feldspar + sphene material is the only evidence of a felsic layer. Clearly, accurate modal analyses of this layer are not possible.

Clinopyroxene + Feldspar + Sphene Layer

This layer consists of a fine-grained granoblastic aggregate of clinopyroxene + K-feldspar + plagioclase + sphene. The clinopyroxene can occur in thin stringers, and sphene commonly shows an alignment parallel to these clinopyroxene stringers. This gives the layer a weak foliation broadly parallel to the layer boundaries. The majority of fine-grained feldspar in this layer is of two types (as determined by microprobe analyses, Section 5.5). These are K-feldspar with Or > 90, and plagioclase with an An content around 90 (anorthite). The plagioclase is typically altered to a very turbid brown appearance, but the K-feldspar is clear. This selective alteration will be discussed in greater detail in Section 5.5. Coarser, subidiomorphic grains of plagioclase (presumably relict) also occur throughout this zone. These grains are commonly twinned and are not as intensely altered as the finer-grained plagioclase. Compositions of these grains range from An 50 to An 75.

Biotite + Feldspar + Sphene Layer

This layer is similar to the previous one except that pale-brown biotite occurs in place of clinopyroxene. This causes a distinct change in the colour of the hand specimen from green to brown. Plagioclase is still strongly altered, in contrast to the clear K-feldspar. A minor foliation exists within this layer, due to the alignment of biotite and sphene.

Biotite + Feldspar Unit

This unit consists of K-feldspar + plagioclase + biotite, and the boundary between it and the biotite + feldspar + sphene layer is marked by the disappearance of sphene and the change in biotite colour from pale brown to red brown. The fine-grained feldspar is mainly K-feldspar Or 90 and plagioclase An 90, though coarser grains of twinned plagioclase

with lower An content are common. Plagioclase alteration is still evident close to the biotite + K-feldspar + sphene layer. However, a distinct boundary within the biotite + feldspar unit, parallel to this layering, is denoted by the limit of this alteration. Microprobe scans across this unit have confirmed the lack of quartz in this assemblage. A weak foliation is defined by poor alignment of the biotite.

Sulphides Within the Layers

Thin lenses of opaque grains, consisting predominantly of chalcopyrite, bornite, and small amounts of pyrite, are common to all the very fine-grained layers. Some lenses parallel the layer boundaries, whereas others cut across them. In that part of the biotite + feldspar unit furthest from the marble, muscovite and occasional grains of green tourmaline are typically associated with the sulphides. Closer to the marble, however, muscovite is replaced by K-feldspar, and this change appears to coincide with the change from unaltered to altered plagioclase. This feature will be discussed further in Section 5.9. The assemblages in these sulphide lenses are recorded as separate from the general assemblages within the layers. Therefore, in the modal analyses (Table 5.1), they are shown as a percentage of the total rock, but are ignored in normalising the layer assemblages to 100%, to allow the general assemblages to be compared directly.

Clinopyroxene + Garnet: Felsic Layer Boundary

This boundary marks a particularly sharp change in mineralogy and texture (noted above), and therefore is most likely to represent the original contact between the two contrasting rock types. It also marks the boundary between the presence and absence of K and Ti, implying that very little diffusion of these elements has occurred into the marble. Traverse 371-VS2 is an exception, though, because a poorly defined thin layer of clinopyroxene + garnet + K-feldspar occurs between the felsic and clinopyroxene + garnet layers (Table 5.1). This clinopyroxene + garnet + K-feldspar layer is similar in grainsize to the clinopyroxene + garnet layer, and seems to suggest that some K diffusion has occurred across the proposed original boundary in this example. This is probably related to the high K-feldspar content of the clinopyroxene + feldspar + sphene layer in this traverse. Patches also occur along the clinopyroxene

+ garnet : felsic layer boundary containing relatively coarse grains of clinopyroxene, garnet, K-feldspar and sphene. These grains, especially sphene, commonly have idioblastic form, and these patches may result from grain growth into original voids.

5.4.3 Garnet-rich Matrix → Pelite Reaction Bands

Traverses 371-1B and 371-VI depict this type of reaction band. The general sequence of layers is:

garnet-rich matrix
garnet + clinopyroxene
felsic (K-feldspar + sphene ± clinopyroxene ± plagioclase)
clinopyroxene + feldspar + sphene
biotite + feldspar + sphene
biotite + feldspar unit.

Garnet-rich Matrix

The matrix consists predominantly (> 70%) of a network of garnet of medium grainsize (1-5 mm). The garnet is typically idioblastic to sub-idioblastic, colourless, varies from isotropic to weakly birefringent, and is commonly optically zoned. Clinopyroxene (not evident in hand specimen) is also a major component, occurring as small grains generally within the garnets. A host of secondary phases occurs interstitially to the garnet. Calcite, in coarse irregularly shaped grains, is the most prominent of these. Calcite also occurs as an alteration product of the garnet. This alteration is commonly restricted to specific concentric zones within the garnet, and, occasionally only the outer shells of the original garnet may remain. Most garnets, however, are unaffected. Secondary sulphide minerals are prominent amongst the garnet. These are dominated by bornite and chalcopyrite, with associated stringers of chalcocite, and small patches of covellite and tetrahedrite (with tennantite solid solution, detected by microprobe analyses). A pale-yellow (in reflected light) sulphide has also been recognised rimming the chalcopyrite and in thin veins. From qualitative microprobe analyses this may be tungstenite. K-feldspar and prehnite have also been noted as secondary phases amongst the garnet.

Garnet + Clinopyroxene Layer

This layer is not as clearly defined in this type of reaction band as in the marble → pelite reaction bands. It occurs as a thin layer

between the garnet-rich matrix and the fine-grained feldspar-rich layers (see below), in which clinopyroxene is typically more abundant than garnet (Table 5.1).

Garnet + Clinopyroxene Layer → Biotite + Feldspar Unit

The sequence of layers between the garnet + clinopyroxene layer and the biotite + feldspar unit (outlined above) is identical to that described in the marble → pelite reaction bands (Section 5.4.2). Again the garnet + clinopyroxene : felsic layer boundary is delineated by a sharp change in grainsize and texture, and is likely to represent the original contact (between a calcareous-rich matrix and the pelite). This boundary, however, is variable, and sharp contacts between the garnet-rich matrix and the clinopyroxene + feldspar + sphene layer are found. Notably, though, where the garnet + clinopyroxene layer is well developed, so is the felsic layer.

A major difference between these two types of reaction band is that the layers within the garnet-rich matrix → pelite reaction bands are much wider than those in the marble → pelite reaction bands. The combined width of the feldspathic layers (the very fine-grained feldspar-containing layers on the pelite side of the proposed original contact) associated with the marble are usually no more than 2 mm wide, whereas these zones associated with the matrix are commonly over 1 cm wide. These wider reaction bands typically show division of the clinopyroxene + feldspar + sphene layer into two distinct sublayers distinguishable in hand specimen by their colour (Section 5.2), with the one closest to the garnet-rich matrix being pale green, the other grey-green (e.g. 371VI, Plate 5-1C). No change in mineral assemblage or mode is evident between the two sublayers. However, within the pale-green sublayer, the plagioclase is strongly altered to a brownish material, whereas in the grey-green sublayer it remains fresh. Similarly, feldspars further from the matrix (i.e. in the biotite + feldspar + sphene layer and the biotite + feldspar unit) are also unaltered. Hence, there appears to be an outer limit to the feldspar alteration. In the marble → pelite reaction bands this limit occurs within the biotite + feldspar unit, but with an increase in the widths of the layers, associated with the matrix → pelite reaction bands, this limit occurs within the clinopyroxene + feldspar + sphene layer.

5.4.4 Garnet-rich Matrix → Marble Reaction Bands

Two types of simple reaction band occur between the garnet-rich matrix and marble, both involving wollastonite. One comprises thin rims of wollastonite (0.5 mm → 2mm) developed within the original outlines of the marble blocks (e.g. traverse 371-1D). The other type is typically more extensive (commonly 1-2 cm wide) and comprises a coarser-grained layer of wollastonite, garnet and lesser amounts of fine-grained clinopyroxene developed between the garnet-rich matrix and marble (e.g. traverse 371-L, Table 5.1).

In thin section, no clear evidence exists for the position of the original contact in the second type of layering, because there is no abrupt change in grainsize. However, from hand specimen, the sharpness of the garnet-rich matrix : wollastonite layer boundary relative to the wollastonite layer : marble boundary suggests that the former is more likely to represent the initial contact.

5.5 MINERAL CHEMISTRY

5.5.1 Introduction

Minerals have been analysed to study variations across the reaction bands, and for calculating, using modal analyses, bulk compositions of the individual layers (Section 5.6). Mineral profiles across selected reaction bands from samples collected at locality 371 are given in Figs. 5-2A→G. Microprobe analyses of phases used in calculating layer compositions are given in Tables 5-2A→E.

5.5.2 Garnet

Garnets from the reaction bands studied in detail are grossular-andradite solid solutions. Representative analyses are shown in Tables 5.2A→E. Based on the end-member calculations of Rickwood (1968), all garnets are classified as grossular, typically ranging from Gr 65 to Gr 85. They contain minor amounts of spessartine (0 - 0.4%) and pyrope (0 - 1.7%), but an almandine component is very rare (garnets with lower grossular values of Gr 50 - Gr 63 and almandine values of 2 - 4% have been recorded

Figure 5-2: Profiles of mineral composition across selected reaction bands. Points represent mineral analyses, and those inside brackets in Figures D and F represent analyses from a single grain. The points are joined to represent the continuous occurrence of the mineral across the reaction band. Garnet and clinopyroxene grains within marble are shown separately.

Figures 5-2A→F show variations in the garnet $Al/Al+Fe^{3+}$ and clinopyroxene Mg/Mg+Fe ratios. Figure 5-2G shows variation in the biotite Al/sum y (sum y = total number of cations in the octahedral layer), Ti/sum y and Mg/Mg+Fe ratios across the reaction band of traverse 371-1A.

Abbreviations: B-F = biotite + feldspar unit, B-F-S = biotite + feldspar + sphene layer, C-F-S = clinopyroxene + feldspar + sphene layer, F = felsic layer, G-K = garnet + K-feldspar layer, G-C = garnet + clinopyroxene layer, G = garnet layer, M = marble, GT-RICH matrix = garnet-rich matrix.

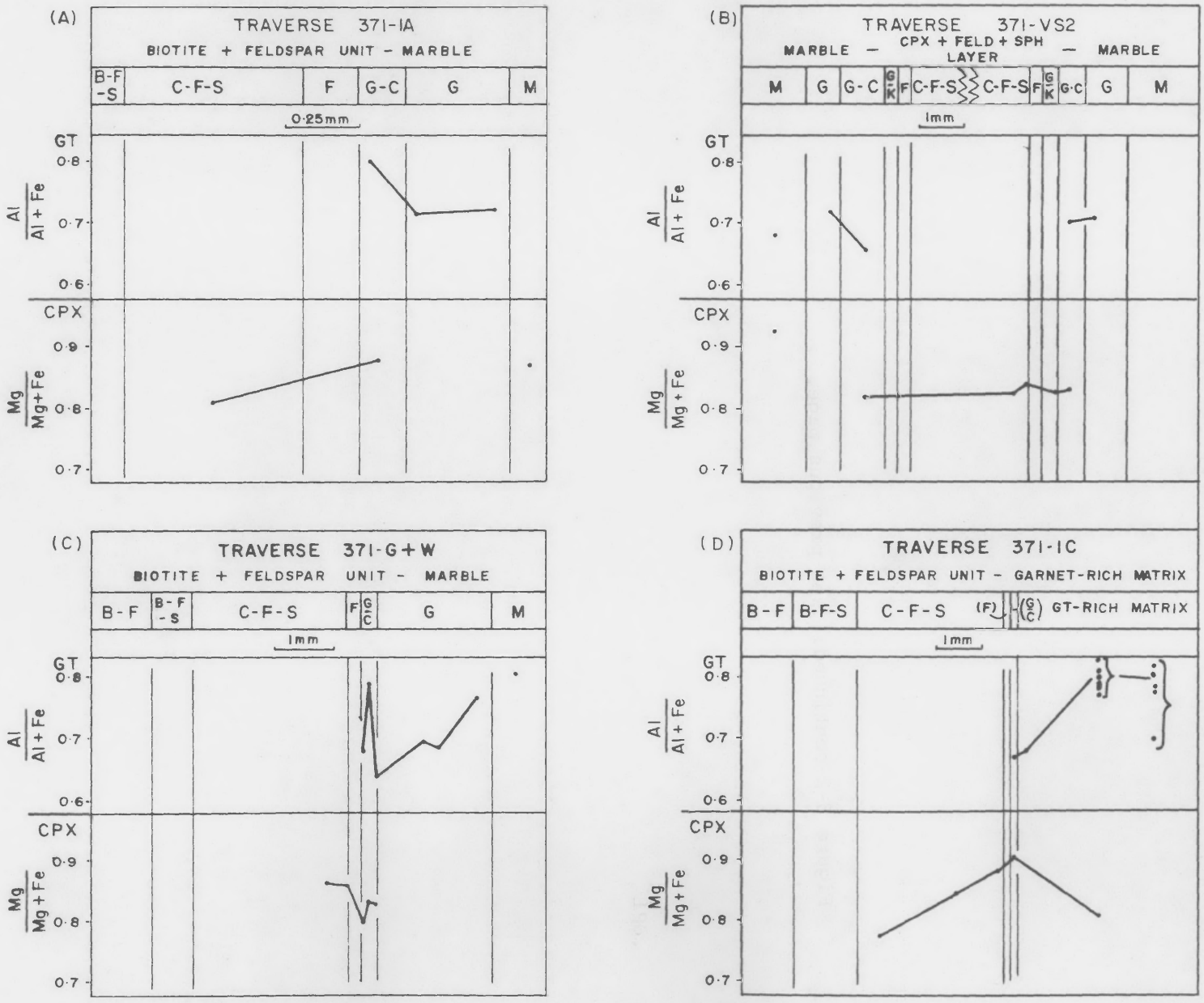
(A)
TRAVERSE 371-1A
BIOTITE + FELDSPAR UNIT - MARBLE
B-F -S
C-F-S
F
G-C
G
M
0·25mm
GT
CPX
Al / Al + Fe
Mg / Mg + Fe
0·8
0·7
0·6
0·9
(B)
TRAVERSE 371-VS2
MARBLE — CPX + FELD + SPH LAYER — MARBLE
M
G
G-C
G-K
F
C-F-S
C-F-S
F
G-K
G-C
G
M
1mm
(C)
TRAVERSE 371-G+W
BIOTITE + FELDSPAR UNIT - MARBLE
B-F
B-F -S
C-F-S
F
G-C
G
M
1mm
(D)
TRAVERSE 371-1C
BIOTITE + FELDSPAR UNIT - GARNET-RICH MATRIX
B-F
B-F-S
C-F-S
(F)
(G-C)
GT-RICH MATRIX
1mm

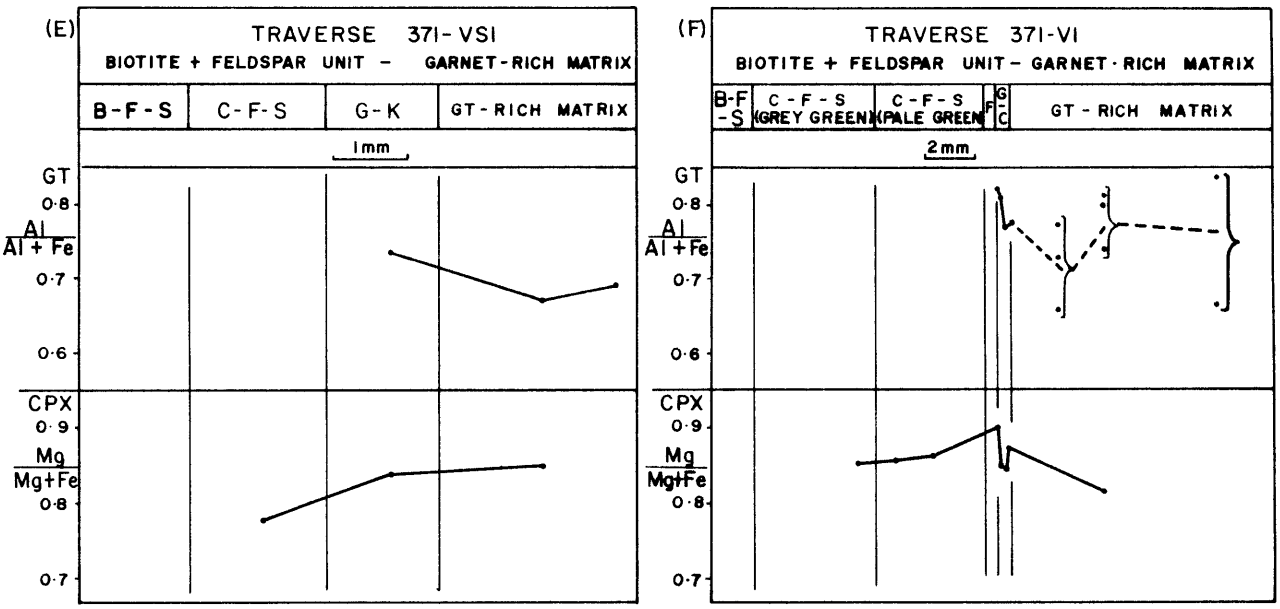
(E)
TRAVERSE 371-VSI
BIOTITE + FELDSPAR UNIT - GARNET-RICH MATRIX
B-F-S
C-F-S
G-K
GT-RICH MATRIX
1mm
GT
0·8
Al / Al+Fe
0·7
0·6
CPX
0·9
Mg / Mg+Fe
0·8
0·7
(F)
TRAVERSE 371-VI
BIOTITE + FELDSPAR UNIT - GARNET-RICH MATRIX
B-F-S
C-F-S (GREY GREEN)
C-F-S (PALE GREEN)
F
G-C
GT-RICH MATRIX
2mm
GT
0·8
Al / Al+Fe
0·7
0·6
CPX
0·9
Mg / Mg+Fe
0·8
0·7

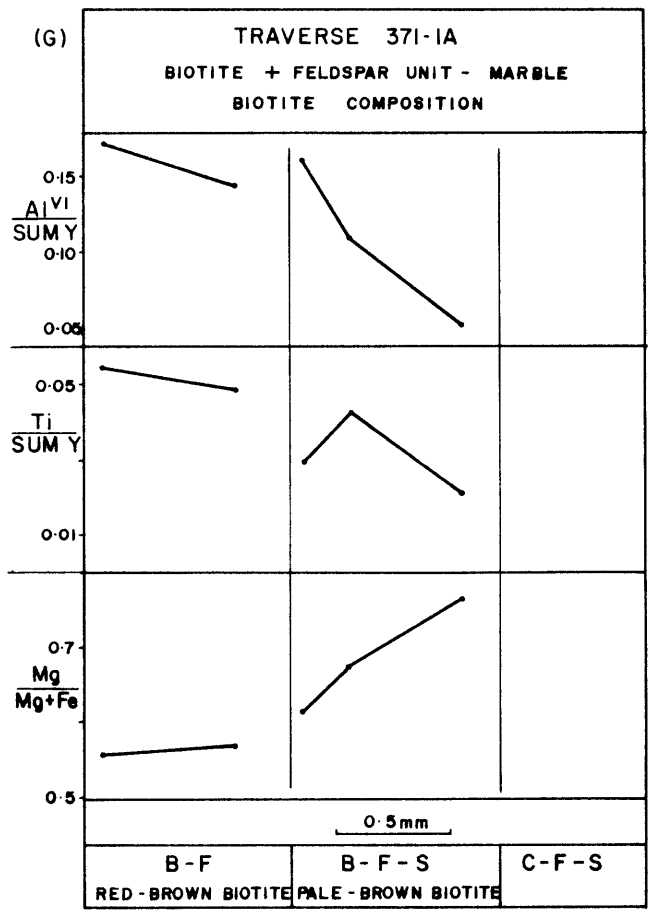
(G)
TRAVERSE 371-IA
BIOTITE + FELDSPAR UNIT - MARBLE
BIOTITE COMPOSITION
0·15
Al VI / SUM Y
0·10
0·05
0·05
Ti / SUM Y
0·01
0·7
Mg / Mg+Fe
0·5
0·5mm
B-F
RED-BROWN BIOTITE
B-F-S
PALE-BROWN BIOTITE
C-F-S

TABLE 5.2A. Typical microprobe analyses from traverse 371-1A

	BI+FELD UNIT			BI+FELD+SPH LAYER			CPX+FELD+SPH LAYER			FELSIC LAYER		GT+CPX LAYER	GT LAYER		MARBLE		
	BI	K-F	PLAG	BI	K-F	PLAG	K-F	PLAG	CPX	K-F	CPX	CPX	GT	GT	CPX	GT	SPH
SiO_2	34.84	As	45.96	34.69	63.03	42.07	59.39	As	53.15	As in		52.96	38.82	38.41	53.68	39.02	30.30
TiO_2	2.44	in	-	1.51	-	[I]0.24	[I]2.45	in	-	the		0.13	1.22	-	-	0.31	35.93
Al_2O_3	20.36	the	25.21	21.01	18.85	26.09	19.78	the	1.20	CPX+		1.26	17.80	16.67	0.38	20.29	2.06
Fe_2O_3	-	BI+FELD+	-	-	-	-	-	BI+FELD	-	FELD+		[*]1.28	[**]6.68	[**]9.71	[*]0.59	[**]3.58	-
FeO	15.79	SPH	0.15	14.28	-	-	-	+SPH	5.90	SPH		3.63	-	-	4.08	-	-
MnO	-	LAYER	-	-	-	-	-	LAYER	-	LAYER		-	0.15	-	0.19	0.12	-
MgO	11.72		-	12.76	-	-	-		13.99			14.77	0.24	-	15.21	0.29	-
CaO	0.11		13.47	0.55	0.18	12.76	0.27		25.26			26.17	36.68	36.56	26.56	37.28	29.28
Na_2O	0.14		0.32	-	0.62	0.86	0.79		-			-	-	-	-	-	-
K_2O	10.48		0.27	9.69	15.88	0.16	13.32		-			-	-	-	-	-	-
Total	95.88		[†]85.38	94.49	98.56	[†]82.18	[†]96.00		99.50			100.20	101.59	101.35	100.69	100.89	97.57
Structural formulae																	
No. of oxygens	22		32	22	32	32	32		6			6	24	24	6	24	10
Si	5.215		9.706	5.208	11.842	9.230	11.380		1.977			1.951	5.887	5.893	1.971	5.894	2.025
Al^{IV}	2.785		6.278	2.792	4.177	6.779	4.471		0.023			0.049	0.113	0.107	0.016	0.106	
Al^{VI}	0.810			0.929					0.030			0.006	3.068	2.908	-	3.506	0.162
Ti	0.275		-	0.171	-	0.040	0.353		-			0.004	0.139	-	-	0.035	1.806
Fe^{3+}	-		-	-	-	-	-		-			0.035	0.762	1.121	0.016	0.407	-
Fe^{2+}	1.977		0.026	1.793	-	-	-		0.184			0.112	-	-	0.125	-	-
Mn	-		-	-	-	-	-		-			-	0.019	-	0.006	0.015	-
Mg	2.615		-	2.855	-	-	-		0.776			0.811	0.054	-	0.833	0.065	-
Ca	0.018		3.048	0.089	0.036	3.012	0.055		1.007			1.033	5.960	6.010	1.045	6.033	2.096
Na	0.041		0.131	-	0.226	0.367	0.294		-			-	-	-	-	-	-
K	2.002		0.073	1.856	3.807	0.045	3.256		-			-	-	-	-	-	-
Total cations	15.738		19.262	15.693	20.088	19.513	19.809		3.997			4.001	16.002	16.039	4.012	16.061	6.089
$Mg/Fe^{2+}+Mg$	0.569			0.614					0.809			0.879			0.869		
$Al^{VI}/Al^{VI}+Fe^{3+}$													0.801	0.722		0.896	
Or			2.24		93.56	1.31	90.32										
Ab			4.03		5.55	10.73	8.14										
An			93.73		0.89	87.96	1.54										

[*]Fe_2O_3 based on 16 cations. [**]Fe_2O_3 calculated by method of Papike *et al.* (1974). [I]Ti impurities, probably sphene.

[†]Low totals due to alteration (see text).

Reaction band abbreviations: BI+FELD UNIT = biotite + feldspar unit, BI+FELD+SPH LAYER = biotite + feldspar + sphene layer, CPX+FELD+SPH LAYER = clinopyroxene + feldspar + sphene layer, CPX+GT LAYER = clinopyroxene + garnet layer, GT LAYER = garnet layer

Mineral abbreviations: BI = biotite, K-F = K-feldspar, PLAG = plagioclase, CPX = clinopyroxene, GT = garnet, SPH = sphene.

TABLE 5.2B. Typical microprobe analyses from traverse 371-VS2

	CPX+FELD+SPH LAYER			FELSIC LAYER			GT+CPX+K-F LAYER			GT+CPX LAYER		GT LAYER
	K-F	PLAG	CPX	K-F	PLAG	CPX	K-F	CPX	GT	CPX	GT	GT
SiO_2	64.19	44.05	52.92	64.35		52.88		52.90		53.63	37.94	38.23
TiO_2	-	-	-	-	As in	-	As in	-	As in	-	0.61	0.86
Al_2O_3	18.74	35.89	1.22	18.79	the	1.71	the	1.37	the	0.78	15.65	15.92
Fe_2O_3	-	-	**2.27	-	CPX+FELD	**1.63	FELSIC	**1.73	GT+CPX	**0.27	*9.78	*9.61
FeO	0.16	-	5.18	-	+SPH	4.70	LAYER	5.03	LAYER	5.46	-	-
MnO	-	-	-	-	LAYER	-		-		-	-	-
MgO	-	-	13.87	-		13.58		13.77		14.74	0.13	-
CaO	0.17	19.25	24.95	0.09		24.82		25.22		25.31	36.43	36.64
Na_2O	0.47	0.57	0.25	0.80		0.41		0.30		-	-	-
K_2O	16.35	-	0.09	15.72		0.21		-		-	-	-
Total	100.08	99.76	100.75	99.75		99.94		100.31		100.19	100.54	101.26
Structural formulae												
No. of oxygens	32	32	6	32	32	6	32	6	24	6	24	24
Si	11.893	8.161	1.953	11.915		1.959		1.957		1.979	5.885	5.881
Al^{IV}	4.094	7.841	0.047	4.103		0.041		0.043		0.021	0.115	0.119
Al^{VI}			0.006			0.034		0.016		0.013	2.746	2.768
Ti	-	-	-	-		-		-		-	0.071	0.100
Fe^{3+}	-	-	0.063	-		0.046		0.048		0.008	1.142	1.113
Fe^{2+}	0.025	-	0.160	-		0.146		0.156		0.168	-	-
Mn	-	-	-	-		-		-		-	-	-
Mg	-	-	0.763	-		0.750		0.759		0.811	0.030	-
Ca	0.034	3.821	0.986	0.018		0.985		1.000		1.001	6.054	6.039
Na	0.169	0.205	0.018	0.287		0.030		0.022		-	-	-
K	3.865	-	0.004	3.714		0.010		-		-	-	-
Total cations	20.080	20.028	4.000	20.037		4.001		4.001		4.001	16.043	16.020
$Mg/Fe^{2+}+Mg$			0.827			0.837		0.830		0.828		
$Al^{VI}/Al^{VI}+Fe^{3+}$											0.706	0.713
Or	95.02	-		92.41								
Ab	4.15	5.09		7.15								
An	0.83	94.91		0.44								

*Fe_2O_3 based on 16 cations. **Fe_2O_3 calculated by method of Papike *et al.* (1974).

Abbreviations shown in Table 5.2A, plus GT+CPX+K-F LAYER = garnet + clinopyroxene + K-feldspar layer

Typical sphene analysis shown in Table 5.2A

TABLE 5.2C. Typical microprobe analyses from traverse 371-1B

	BI+FELD LAYER			BI+FELD+SPH LAYER			CPX+FELD+SPH LAYER			FELSIC LAYER		GT+CPX LAYER		GT MATRIX	
	BI	K-F	PLAG	BI	K-F	PLAG	K-F	PLAG	CPX	K-F	CPX	CPX	GT	CPX	GT
SiO_2	33.61			35.79	63.62	45.84	60.54	45.57	53.89			53.28	37.99	52.70	38.57
TiO_2	2.74	As in the		2.20	-	-	[I] 1.80	-	-	As in the		-	-	-	0.59
Al_2O_3	22.41	BI+FELD+SPH		18.74	18.58	26.62	19.64	25.38	0.78	CPX+FELD+SPH		0.77	15.57	0.60	17.93
Fe_2O_3	-	LAYER		-	-	-	-	-	-	LAYER		[*] 1.21	[**] 10.96	[*] 1.38	[**] 6.69
FeO	15.69			12.93	-	-	-	-	4.96			2.82	-	5.85	-
MnO	-			-	-	-	-	-	-			-	-	-	-
MgO	10.97			14.79	-	-	-	-	14.94			15.47	-	13.44	0.15
CaO	0.14			-	-	13.12	0.20	12.74	25.52			26.04	36.36	25.61	36.95
Na_2O	-			-	0.47	0.28	0.73	-	-			-	-	0.17	-
K_2O	10.35			10.60	15.86	0.37	13.94	0.17	-			-	-	-	-
Total	95.91			95.05	98.53	[+]86.23	[+]96.85	[+]83.86	100.09			99.59	100.88	99.75	100.88
Structural formulae															
No. of oxygens	22			22	32	32	32	32	6			6	24	6	24
Si	5.023			5.333	11.929	9.568	11.509	9.737	1.985			1.966	5.889	1.970	5.893
Al^{IV}	2.977			2.667	4.108	6.552	4.403	6.394	0.015			0.034	0.111	0.026	0.107
Al^{VI}	0.974			0.627					0.019			-	2.733	-	3.121
Ti	0.308			0.246	-	-	0.257	-	-			-	-	-	0.068
Fe^{3+}	-			-	-	-	-	-	-			0.034	1.279	0.039	0.769
Fe^{2+}	1.961			1.611	-	-	-	-	0.153			0.087	-	0.183	-
Mn	-			-	-	-	-	-	-			-	-	-	-
Mg	2.444			3.284	-	-	-	-	0.820			0.851	-	0.749	0.034
Ca	0.022			-	-	2.934	0.041	2.917	1.007			1.030	6.039	1.026	6.048
Na	-			-	0.171	0.113	0.269	-	-			-	-	0.012	-
K	1.974			2.015	3.795	0.099	3.382	0.046	-			-	-	-	-
Total cations	15.683			15.784	20.003	19.266	19.861	19.094	3.999			4.002	16.051	4.005	16.040
$Mg/Fe^{2+}+Mg$	0.555			0.671					0.843			0.907		0.804	
$Al^{VI}/Al^{VI}+Fe^{3+}$													0.681		0.802
Or					95.69	3.13	91.61	1.56							
Ab					4.31	3.60	7.29	-							
An					-	93.27	1.10	98.44							

[*] Fe_2O_3 based on 16 cations. [**] Fe_2O_3 calculated by method of Papike *et al.* (1974). [I] Ti impurities, probably sphene.

[+] Low totals due to alteration (see text).

Abbreviations shown in Table 5.2A plus GT MATRIX = garnet-rich matrix.

Typical sphene analysis shown in Table 5.2A.

TABLE 5.2D. Typical microprobe analyses from traverse 371-VI

	BI+FELD+SPH LAYER			CPX+FELD+SPH LAYER			FELSIC LAYER			GT+CPX LAYER		GT MATRIX	
	BI	K-F	PLAG	K-F	PLAG	CPX	K-F	PLAG	CPX	CPX	GT	CPX	GT
SiO_2	36.35	62.55	46.04	61.72	47.18	53.73	62.37		53.65	53.69	38.22	53.11	38.70
TiO_2	1.18	[I] 1.16	-	[I] 0.73	[I] 0.15	-	[I] 0.80	As in	-	-	1.14	-	0.16
Al_2O_3	18.53	18.37	35.00	19.97	33.74	0.88	18.81	the	0.61	0.96	16.92	0.71	18.32
Fe_2O_3	-	-	-	-	-	[**] 0.08	-	CPX+	[**] 0.54	[**] 0.49	[*] 7.43	[**] 1.11	[*] 6.94
FeO	12.22	0.13	-	-	-	4.61	-	FELD+	4.62	4.76	-	5.47	-
MnO	-	-	-	-	-	-	-	SPH	-	-	0.17	-	-
MgO	16.28	-	-	-	-	14.97	-	LAYER	14.93	14.73	0.23	13.90	0.17
CaO	0.48	1.36	18.28	0.81	16.68	25.75	0.35		25.71	25.91	36.46	26.03	36.60
Na_2O	-	0.61	1.02	1.11	1.19	-	0.96		-	-	-	-	-
K_2O	9.12	15.31	0.33	13.70	1.25	-	14.87		-	-	-	-	-
Total	94.16	99.49	100.67	98.04	100.19	100.02	98.16		100.05	100.54	100.57	100.33	100.89
Structural formulae													
No. of oxygens	22	32	32	32	32	6	32		6	6	24	6	24
Si	5.401	11.689	8.431	11.582	8.674	1.979	11.741		1.979	1.972	5.880	1.968	5.904
Al^{IV}	2.599	4.048	7.558	4.419	7.315	0.021	4.175		0.021	0.028	0.120	0.031	0.097
Al^{VI}	0.649					0.018			0.006	0.014	2.948	-	3.197
Ti	0.132	0.163	-	0.103	0.021	-	0.113		-	-	0.132	-	0.018
Fe^{3+}	-	-	-	-	-	0.002	-		0.015	0.013	0.860	0.031	0.797
Fe^{2+}	1.519	0.020	-	-	-	0.142	-		0.143	0.145	-	0.170	-
Mn	-	-	-	-	-	-	-		-	-	0.022	-	-
Mg	3.605	-	-	-	-	0.822	-		0.821	0.807	0.053	0.768	0.039
Ca	0.076	0.272	3.587	0.163	3.286	1.016	0.071		1.016	1.019	6.010	1.034	5.982
Na	-	0.221	0.362	0.404	0.424	-	0.350		-	-	-	-	-
K	1.729	3.651	0.077	3.280	0.293	-	3.572		-	-	-	-	-
Total cations	15.710	20.064	20.015	19.951	20.013	4.000	20.022		4.001	4.000	16.025	4.002	16.034
$Mg/Fe^{2+}+Mg$	0.704					0.853			0.852	0.846		0.819	
$Al^{VI}/Al^{VI}+Fe^{3+}$							-				0.774		0.801
Or		88.10	1.92	85.27	7.32		89.46						
Ab		5.33	9.00	10.50	10.60		8.78						
An		6.57	89.08	4.23	82.08		1.76						

[*] Fe_2O_3 based on 16 cations. [**] Fe_2O_3 calculated by method of Papike *et al.* (1974). [I] Ti impurities, probably sphene.

Abbreviations shown in Table 5.2A plus GT MATRIX = garnet-rich matrix.

Typical sphene analysis shown in Table 5.2A.

TABLE 5.2E. Typical microprobe analyses from traverse 371-L

	GT MATRIX		WOLL LAYER		MARBLE	
	CPX	GT	CPX	GT	CPX	GT
SiO_2	53.46	38.49	54.14	38.83		
TiO_2	-	0.28	-	0.47	AS IN THE	
Al_2O_3	0.59	16.81	0.29	17.44	WOLL	
Fe_2O_3	**0.38	*8.31	**0.45	*7.89	LAYER	
FeO	4.78	-	2.77	-		
MnO	0.22	0.19	0.19	-		
MgO	14.44	-	16.17	-		
CaO	25.93	36.35	26.34	36.75		
Na_2O	-	-	-	-		
K_2O	-	-	-	-		
Total	99.81	100.43	100.36	101.38		
Structural formulae						
No. of oxygens	6	24	6	24		
Si	1.981	5.937	1.979	5.918		
Al^{IV}	0.019	0.063	0.013	0.082		
Al^{VI}	0.007	2.992	-	3.050		
Ti	-	0.033	-	0.054		
Fe^{3+}	0.011	0.965	0.013	0.905		
Fe^{2+}	0.148	-	0.085	-		
Mn	0.007	0.025	0.006	-		
Mg	0.798	-	0.881	-		
Ca	1.030	6.007	1.032	6.001		
Na	-	-	-	-		
K	-	-	-	-		
Total cations	4.001	16.022	4.009	16.010		
$Mg/Fe^{2+}+Mg$	0.843		0.912			
$Al^{VI}/Al^{VI}+Fe^{3+}$		0.756		0.771		

* Fe_2O_3 based on 16 cations.

** Fe_2O_3 calculated by method of Papike *et al.* (1974).

Abbreviations: GT MATRIX = garnet-rich matrix.

WOLL. LAYER = wollastonite layer.

CPX = clinopyroxene, GT = garnet.

from very thin lenses, less than 0.01 mm wide, of calcareous material occurring sporadically within the feldspathic units of 371-VS).

As noted in Section 5.4, the garnets are typically colourless (though they occasionally show a pale-brown tinge), range from isotropic to weakly birefringent, and commonly show optical zoning defined by changes in birefringence. Several detailed microprobe profiles were taken across well zoned garnet grains. Although minor variations in chemistry are common within a single grain (e.g. variation in Al/Al+Fe ratios is typically greater than 0.1) no consistent relation between chemistry and optical zoning are evident.

From the profiles of Figs. 5-2A→F, no consistent trends in garnet chemistry across the layers can be substantiated. Possible systematic variations could be suggested for individual profiles, but these are no greater than variations found within single grains, as emphasised by traverses 371-1C and 371-VI (Figs. 5-2D and F). Inconsistent profiles, with inhomogeneities over small domains, were also found in garnet compositional trends across reaction bands by Kerrick (1977).

Variations in garnet chemistry relative to their optical properties are discussed further in Section 5.11, with reference to a greater range in garnet composition.

5.5.3 Clinopyroxene

Representative clinopyroxene analyses are shown in Tables 5.2A→E. Clinopyroxenes within the reaction bands of locality 371 are typically pale-green to colourless diopside-hedenbergite solid solutions, with Mg/Mg+Fe ratios varying from 0.77 to 0.91 (the variation is greater for clinopyroxene within the blocks of marble). The clinopyroxene compositional profiles of Fig. 5-2A→F depict inconsistent trends and sharp discontinuities between closely occurring grains, and in this respect they are similar to the profiles of garnet A/Al+Fe ratios (described above). It is possible that the Mg/Mg+Fe ratios of the clinopyroxenes slightly increase across the clinopyroxene + feldspar + sphene layer toward the marble side of the reaction band (e.g. traverses 371-1C and 371-VI), but insufficient data are available to verify this possibility. No consistent change in clinopyroxene Mg/Mg+Fe ratio is obvious across the clinopyroxene + feldspar

+ sphene : felsic layer boundary, or the felsic : garnet + clinopyroxene layer boundary.

5.5.4 Biotite

The change in biotite colour from red-brown in the biotite + feldspar unit to pale-brown in the biotite + feldspar + sphene layer is associated with a general decrease in biotite Ti content. This decrease in Ti is associated with an increase in the biotite Mg/Mg+Fe ratio. However, the negative correlation between these values also depends on the Al content of the biotite, as expressed by the inverse relationship between Ti and Al^{VI} and the Mg/Mg+Fe ratio of biotite, as found by Gorbatschev (1968,1977). These changes in biotite chemistry are shown in Fig. 5-2G for the traverse 371-1A. Representative biotite analyses are shown in Tables 5.2A→E.

5.5.5 Feldspar

Feldspar compositions have been mentioned in Section 5.4.2 above. Two major types of feldspar, K-feldspar Or 90 and plagioclase An 90, occur within the feldspathic layers. Both types are extremely fine-grained and lack twinning. Coarser-grained twinned plagioclase (An 50 - An 75) also occurs sporadically throughout the fine-grained material.

Alteration of the anorthite to a brownish material has been described in Section 5.4. In the thin marble → pelite reaction bands, the alteration extends into the biotite + feldspar unit, but in the wider layers of the garnet-rich matrix → pelite reaction bands the alteration extends only into the clinopyroxene + feldspar + sphene layer. Analyses of the altered anorthite are given in Tables 5.2A→D. The more-altered grains (e.g. 371-1B, #7 and #8, Table 5.2C) typically have low totals ranging from 82 to 87 weight percent, presumably reflecting a high volatile component. The alteration product could be a zeolite (possibly scolecite), with the water being derived from the conversion of original hydrous phases to calc-silicates. The alteration, however, appears to be related to distance from the marble (i.e., in the wider layers only that part of the clino-pyroxene + feldspar + sphene layer closest to the marble contains altered feldspar). Therefore, the introduction of CO_2, from the breakdown of calcite, could also be responsible for the alteration of the feldspar, with the formation of a carbonate alteration product (possibly scapolite).

Identification of the volatile component is required before this alteration can be identified.

5.5.6 Other Phases

Wherever analysed, calcite was found to be virtually pure $CaCO_3$. Similarly wollastonite is essentially pure $CaSiO_3$, with minor Fe present only occasionally. The composition of sphene does not vary. Characteristically, it lacks both Fe and Mn, with only minor Al substitution for Ti. A typical analysis of sphene is given in Table 5.2A.

5.6 CHEMICAL VARIATION ACROSS THE REACTION BANDS

5.6.1 Layer Compositions

Because the layers are extremely narrow, separate chemical analyses were not possible, and mineral and modal analyses from the different layers have been used to investigate the variation in chemistry across the reaction bands. This method is based on that of Thompson (1975a). Modal analyses of the various zones are presented in Table 5.1. The mineral chemistry has been discussed in Section 5.5 and selected analyses used in deriving the bulk compositions are shown in Tables 5.2A→E. Since only minor variations exist in either the modal or mineral analyses within a given layer (Sections 5.4 and 5.5), each calculation is representative of the entire layer.

An example of calculations used to derive the bulk compositions of the layers is given for the garnet + clinopyroxene layer in traverse 371-1A, at the bottom of Table 5.4. Following Thompson (1975a), calculations of the number of moles of individual minerals are based on volumes of 100 cm^3. Therefore, the modal amounts are simply converted to number of moles per 100 cm^3 by dividing by the molar volumes (cm^3) of the phases concerned. The molar volumes used are shown in Table 5.3. These values have been adjusted for solid solution in the plagioclase, clinopyroxene and garnet, using the average compositions shown in Table 5.3. The molar volumes used for biotite (of two different colours) are those of Vernon (1978, Table 2). The number of moles of a particular oxide per 100 cm^3 is then calculated from these molar amounts of the phases per 100 cm^3 and the individual

TABLE 5.3. Molar volumes (cm^3) used in calculating Table 5.4.

Pale-Brown Biotite	304.00
Red-Brown Biotite	304.63
K-Feldspar	106.85
Plagioclase (An 90)	100.69
Sphene	55.65
Clinopyroxene ($Mg/Mg+Fe^{2+}$ = 0.85)	67.06
Garnet ($Al^{VI}/Al^{VI}+Fe^{3+}$ = 0.75)	127.02
Wollastonite	38.72
Calcite	36.87

TABLE 5.4. Moles of oxide constituents per 100 cm^3 within the layers of the calc-silicate reaction bands

	SiO_2	TiO_2	Al_2O_3	Fe_2O_3	FeO	MnO	MgO	CaO	Na_2O	K_2O	H_2O	CO_2
371-1A												
MARBLE	0.2156	0.0008	0.0428	0.0051	0.0049	0.0006	0.0341	2.6621				2.4795
GT	2.3183	-	0.5935	0.2207	-	-	-	2.3658	-	-	-	-
GT+CPX	2.7788	0.0167	0.1699	0.0534	0.1302	0.0016	0.9476	1.7178	-	-	-	-
FELSIC	2.6528	0.2099	0.3593	-	0.0684	-	0.2885	0.5636	0.0227	0.2494	0.0863	-
CPX+FELD+SPH	2.5820	0.1290	0.4125	-	0.1029	-	0.4339	0.9657	0.0225	0.0823	0.0715	
BI+FELD+SPH	2.1961	0.1163	0.6234	-	0.2015	-	0.3209	0.3738	0.0222	0.2244	0.2786	-
BI+FELD	2.1147	0.0450	0.6427	-	0.3257	-	0.4278	0.2736	0.0130	0.2318	0.3272	-
371-VS2												
MARBLE								2.7122				2.7122
GT	2.3151	0.0394	0.5684	0.2189	-	-	-	2.3773	-	-	-	-
GT+CPX	2.6772	0.0122	0.2573	0.1005	0.1420	-	0.6926	1.8768	-	-	-	-
CPX+GT+K-F	2.6026	0.0132	0.4026	0.1146	0.0620	-	0.3074	1.5106	0.0089	0.1159	-	-
FELSIC	2.6090	0.1124	0.4617	0.0064	0.0410	-	0.2081	0.5765	0.0277	0.2470	0.0623	-
CPX+FELD+SPH	2.6853	0.1030	0.3857	0.0123	0.0651	-	0.2942	0.5924	0.0035	0.2654	0.0571	-
371-1B												
GT MATRIX	2.4238	0.0223	0.5317	0.2567	0.0459	-	0.1991	2.2376	0.0015	-	-	-
GT+CPX	2.7036	-	0.2240	0.1095	0.1910	-	0.7972	1.8486	-	-	-	-
FELSIC	2.7659	-	0.3810	-	0.0625	-	0.3348	0.4182	0.0228	0.2873	-	-
CPX+FLED+SPH	2.6181	0.0907	0.4489	-	0.0700	-	0.3752	0.8512	0.0078	0.0998	0.0502	-
BI+FELD+SPH	2.2402	0.1247	0.5878	-	0.1811	-	0.3691	0.3552	0.0010	0.2352	0.2786	-
BI+FELD	2.0741	0.0504	0.6828	-	0.3208	-	0.3998	0.2630	0.0079	0.2305	0.3272	-
371-VI												
GT MATRIX	2.4069	0.0060	0.5638	0.1388	0.0343	-	0.1685	2.4135	-	-	-	-
GT+CPX	2.7176	0.0017	0.2352	0.0665	0.1390	0.0031	0.7823	1.8207	-	-	-	-
FELSIC	2.5335	0.0125	0.5332	0.0015	0.0277	-	0.1593	0.4542	0.0377	0.2415	0.0069	
CPX+FELD+SPH	2.4315	0.1392	0.5420	0.0004	0.0529	-	0.3062	0.9330	0.0340	0.0909	0.0771	
BI+FELD+SPH	2.1465	0.1343	0.6716	-	0.1168	-	0.2747	0.5761	0.0267	0.1685	0.2212	
371-L												
MARBLE	0.5667	0.0040	0.1164	0.0339	0.0055	0.0004	0.0572	2.5955				2.0841
WOLL	2.5026	0.0090	0.2617	0.0761	0.0093	0.0007	0.0962	2.4131	-	-	-	-
GT MATRIX	2.4390	0.0112	0.5055	0.1599	0.0364	0.0100	0.1961	2.2280	-	-	-	-
371-1D												
MARBLE	-	-	-	-	-	-	-	2.7122	-	-	-	2.7122
WOLL	2.5826	-	-	-	-	-	-	2.5826	-	-	-	-
GT MATRIX	2.4238	0.0223	0.5317	0.2567	0.0459	-	0.1991	2.2376	0.0015	-	-	-

EXAMPLE OF CALCULATIONS USED TO DERIVE THIS TABLE

371-1A	MINERALS	MODAL %	MOLAR VOLUMES	MOLES per 100 cm^3	MOLES OF OXIDE CONSTITUENTS PER MOLE OF MINERAL							
					SiO_2	TiO_2	Al_2O_3	Fe_2O_3	FeO	MnO	MgO	CaO
CPX+GT ZONE												
	CPX	77.97	67.06	1.1627	1.9510	0.0040	0.0275	0.0175	0.1120	-	0.8110	1.0330
	GT	22.03	127.02	0.1734	2.9435	0.0695	0.7953	0.1905	-	0.0095	0.0270	2.9800
					2.7788	0.0167	0.1699	0.0534	0.1302	0.0016	0.9476	1.7178

= Moles of oxide constituents per 100 cm^3 in the GT+CPX layer

Modal analyses are shown in Table 5.1. Molar volumes used are shown in Table 5.3. Moles of oxide constituents per mole of mineral are derived from the mineral analyses shown in Table 5.2A-E. Abbreviations shown in Table 5.1.

mineral analyses. The structural formulae of the minerals used are shown in Tables 5.2A→E. Allowing for the number of cations per oxide, the number of moles of oxide per mole of phase can be simply derived. (Note that the structural formulae must be based on the same number of oxygens as the general formulae used in calculating the molar volumes.) For each oxide, the number of moles of oxide present in each mole of phase is multiplied by the number of moles per 100 cm^3 of that phase in the layer to calculate the number of moles of oxide contributed to the layer by each phase. Addition of these values for the different phases within a layer derives the number of moles of oxide per 100 cm^3. This is carried out for each oxide to give the bulk composition of the layer. Table 5.4 is the complete accumulation of such calculations for each layer in the six traverses studied in detail. The data from this table are represented in Figs. 5-3A→F.

5.6.2 Chemical Trends

Several trends are recognised from the traverses portrayed in Figs. 5-3A→D. The most apparent is the stepwise decrease in CaO across the reaction bands. This stepwise change in composition within reaction bands has been described by several authors (e.g. Thompson, 1959; Joesten, 1974). CaO content in the felsic layer does not fit the general trend. However, this may be due to lack of accurate modal data on this layer (Section 5.4). Because of the uncertainties associated with the felsic layer it is only briefly dealt with in this section; it is discussed further in Section 5.9.5. SiO_2, in contrast to CaO, shows no consistent change but tends to maintain high values throughout (excluding the marble). The highest values of SiO_2 are commonly recorded in the clinopyroxene + garnet layer. Al_2O_3 typically decreases (stepwise) toward the Ca-rich ends of the reaction bands, but increases sharply at the garnet layer (or garnet-rich matrix, depending on the traverse being considered). FeO decreases stepwise across the feldspathic layers with increasing CaO, and then increases sharply in the clinopyroxene + garnet layer. MgO has a similar trend to FeO except that MgO increases in the clinopyroxene + feldspar + sphene layer relative to the biotite + feldspar + sphene layer. The increase in MgO is in accord with the higher Mg/Mg+Fe value of clinopyroxene compared to biotite. K_2O decreases sharply across the boundary marking the replacement of biotite by clinopyroxene, but is enriched in

Figure 5-3: Concentration of oxide components (moles per 100 cm^3) across selected reaction bands. These figures are constructed from the data of Table 5.4. For calculations used to derive these data see discussion in the text and a worked example in Table 5.4.

Abbreviations: B-F = biotite + feldspar unit, B-F-S = biotite + feldspar + sphene layer, C-F-S = clinopyroxene + feldspar + sphene layer, F = felsic layer, G-K = garnet + K-feldspar layer, G-C = garnet + clinopyroxene layer, G = garnet layer, M = marble, GT-RICH MATRIX = garnet-rich matrix, W = wollastonite layer.

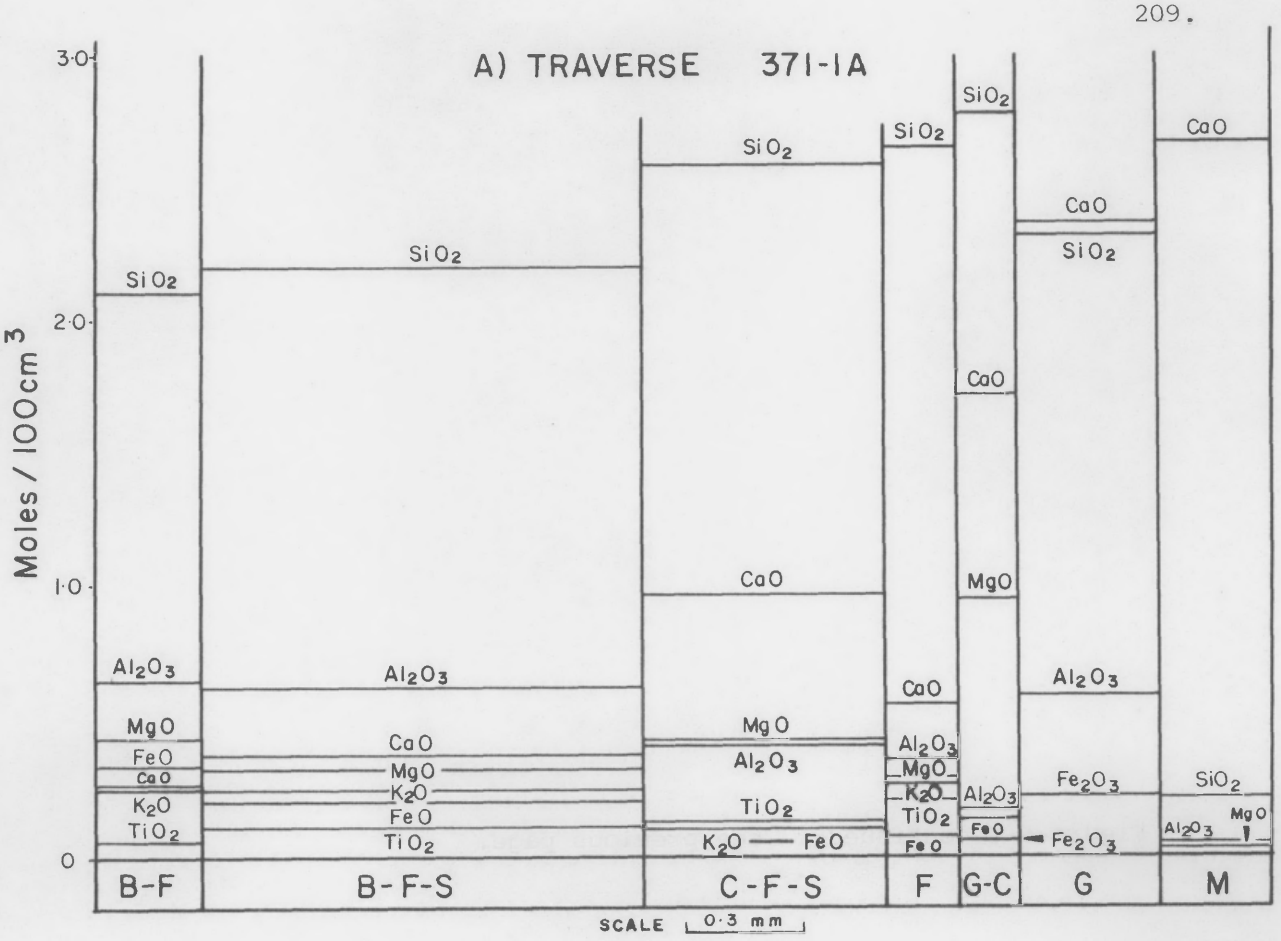
A) TRAVERSE 371-1A
Moles / 100cm3
3·0
2·0
1·0
0
B-F
B-F-S
C-F-S
F
G-C
G
M
SiO2
Al2O3
MgO
FeO
CaO
K2O
TiO2
SCALE 0·3 mm

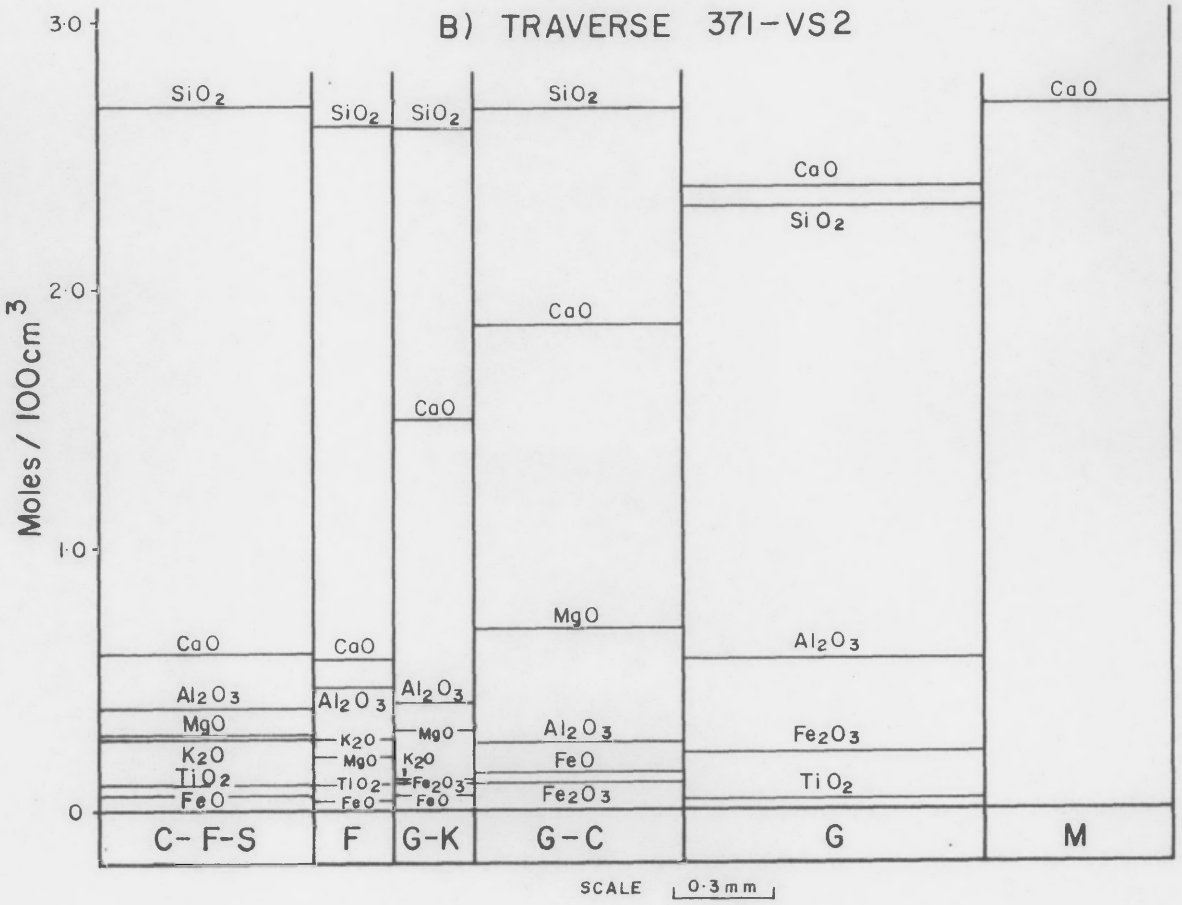
B) TRAVERSE 371-VS2
Moles / 100cm3
3·0
2·0
1·0
0
C-F-S
F
G-K
G-C
G
M
SiO2
CaO
Al2O3
MgO
K2O
TiO2
Fe2O3
FeO
SCALE 0·3 mm

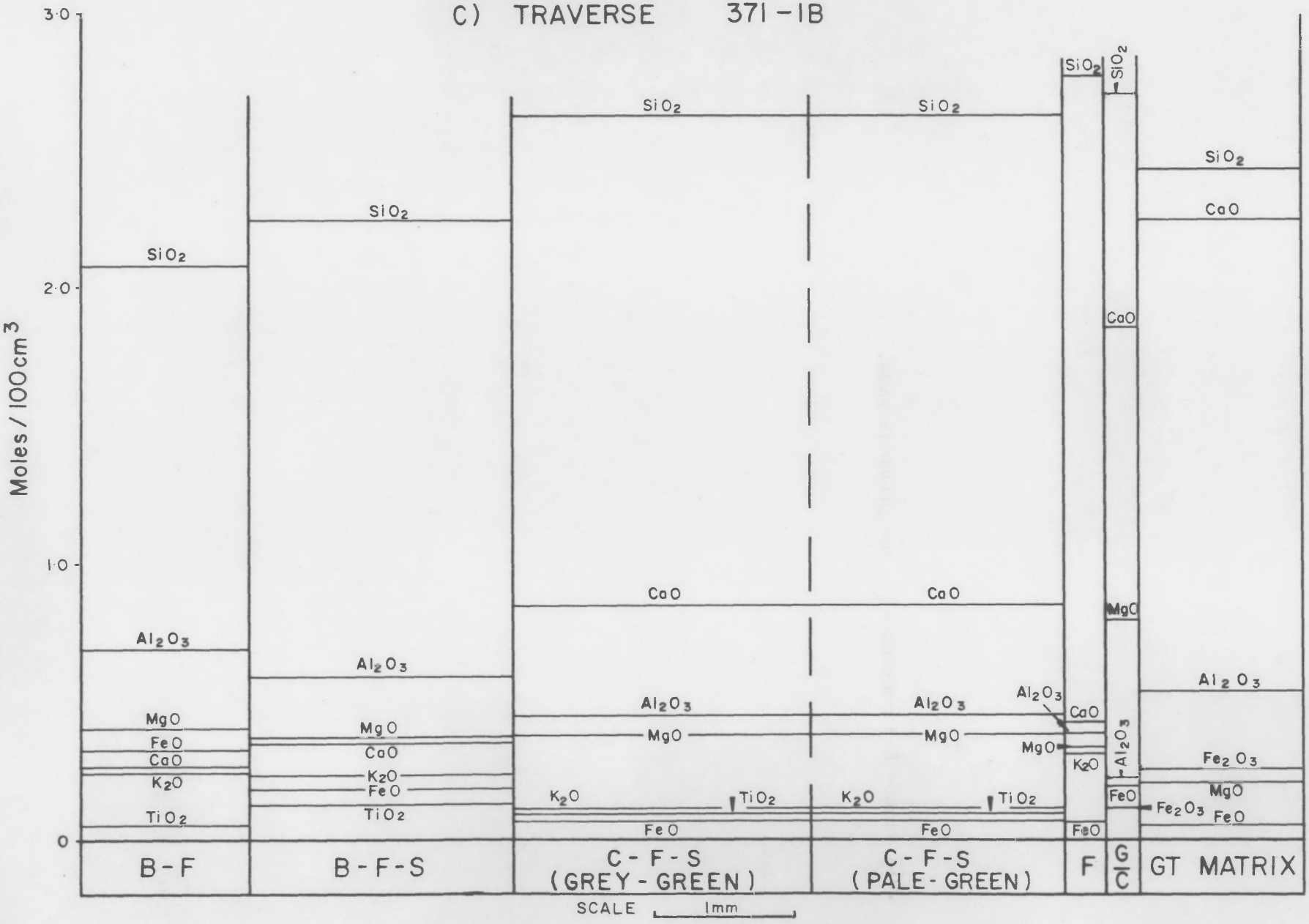
C) TRAVERSE 371-1B
Moles / 100cm3
3·0
2·0
1·0
0
SiO2
Al2O3
MgO
FeO
CaO
K2O
TiO2
B-F
B-F-S
C-F-S (GREY-GREEN)
C-F-S (PALE-GREEN)
F
G/C
GT MATRIX
SCALE 1mm

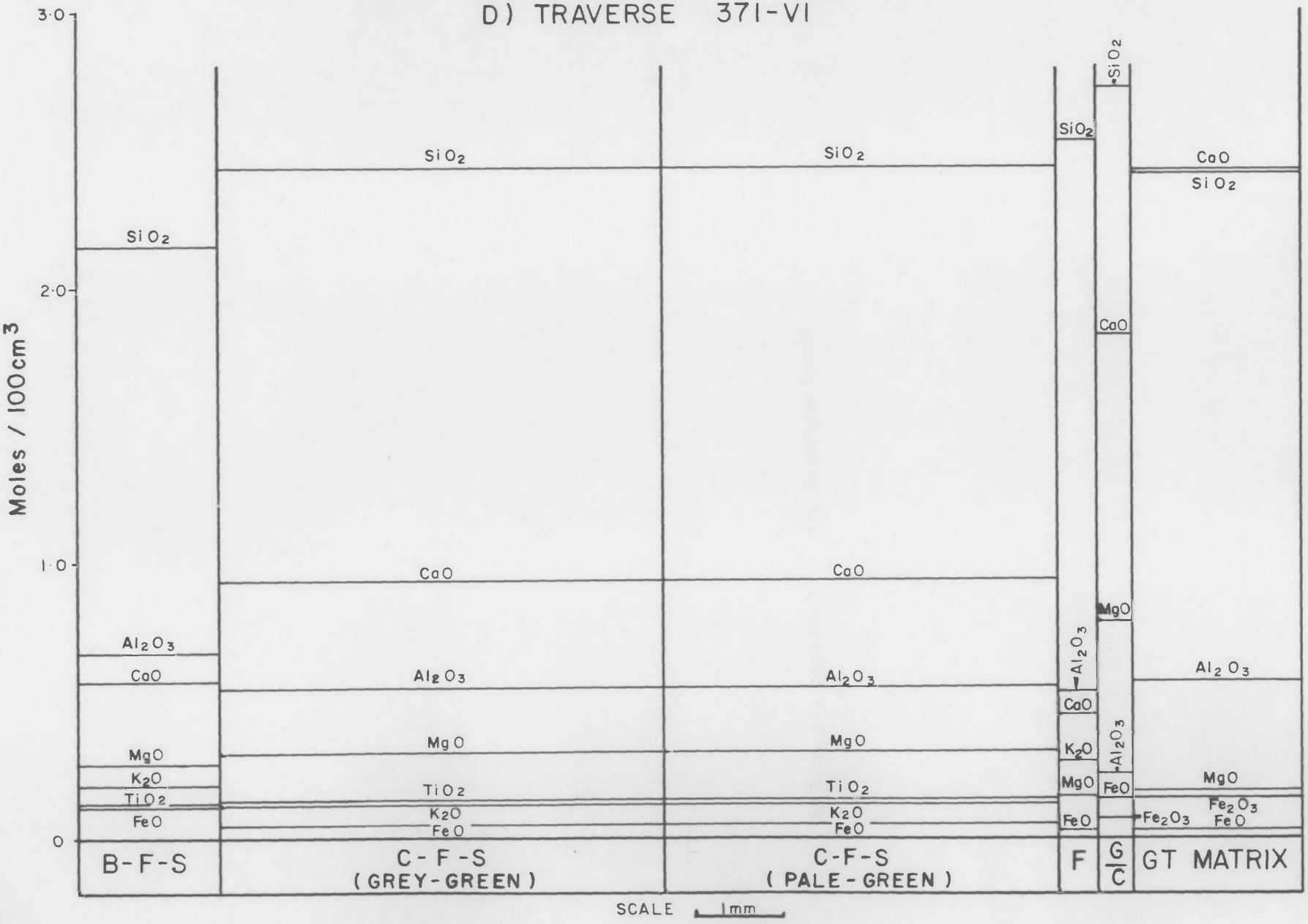
D) TRAVERSE 371-VI
Moles / 100cm3
3·0
2·0
1·0
0
B-F-S
C-F-S (GREY-GREEN)
C-F-S (PALE-GREEN)
F
G/C
GT MATRIX
SiO2
CaO
Al2O3
MgO
K2O
TiO2
FeO
Fe2O3
SCALE 1mm

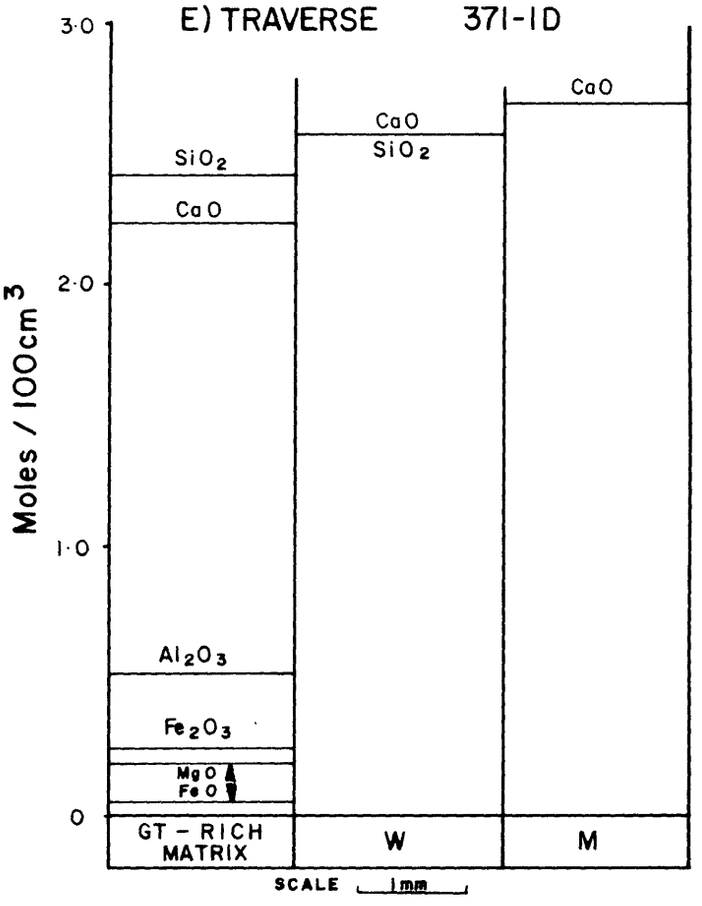
E) TRAVERSE 371-1D
3·0
2·0
1·0
0
Moles / 100cm3
SiO2
CaO
Al2O3
Fe2O3
MgO
FeO
CaO
SiO2
CaO
GT - RICH MATRIX
W
M
SCALE 1mm

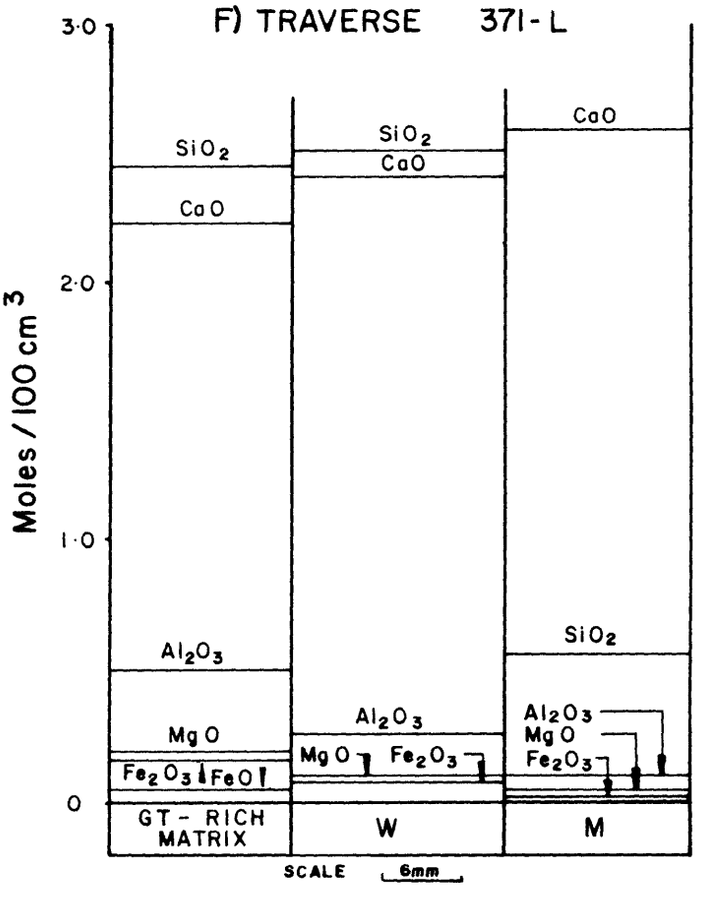
F) TRAVERSE 371-L
3·0
2·0
1·0
0
Moles / 100 cm3
SiO2
CaO
Al2O3
MgO
Fe2O3
FeO
SiO2
CaO
Al2O3
MgO
Fe2O3
CaO
SiO2
Al2O3
MgO
Fe2O3
GT - RICH MATRIX
W
M
SCALE 6mm

the felsic layer relative to the clinopyroxene + feldspar + sphene layer. The thin rim of K-feldspar + sphene noted at the felsic : clinopyroxene + garnet layer boundary (Section 5.4) is not included in these data. Therefore, higher values of K_2O and especially TiO_2 should be shown in the felsic layer (or at least at the felsic : clinopyroxene + garnet layer boundary). An increase in TiO_2 is shown in the sphene-bearing layers compared to the biotite + feldspar unit. This is questionable, however, because an exceptionally fine Ti-bearing phase (e.g. ilmenite, rutile) may well occur in the biotite + feldspar unit unrecorded in the modal analyses (this is discussed further in Sections 5.8 and 5.9).

Several of the features described here agree with those recorded by Thompson (1975a,Fig. 4C). These include the stepwise increase in CaO toward the marble, the maintenance of high SiO_2 values across the layers, and the sharp increase in Al_2O_3 in the garnet layer relative to the clinopyroxene-bearing layers.

The two diagrams of Fig. 5-3E represent examples of the wollastonite layer occurring between the garnet-rich matrix and marble. There is a greater mixture of components in the wollastonite zone of traverse 371-L than that of traverse 371-1D, the latter consisting of only CaO and SiO_2 (i.e. pure wollastonite).

5.6.3 ACF Diagrams

Layer compositions from the traverses shown in Figs. 5-3A→D are plotted in ACF diagrams, Figs. 5-4A→D respectively. The felsic layers are not plotted because of the uncertainties described above. These ACF diagrams emphasise the changes in chemistry across the reaction bands with respect to $Al_2O_3 + Fe_2O_3$ (A), CaO (C) and FeO + MgO (F). Lines drawn between individual layer compositions merely link the plots in sequence across the reaction bands, and are not intended to represent continuous changes in composition (i.e. sharp changes in composition occur across the reaction bands as shown in Figs. 5-3A→D).

The general trend of increasing C relative to A and F across the reaction band is evident in all four ACF diagrams. However, the variation in layer composition cannot be simply related to changes in CaO, because F/F+A ratios are not constant across the reaction bands. Similarly, layer

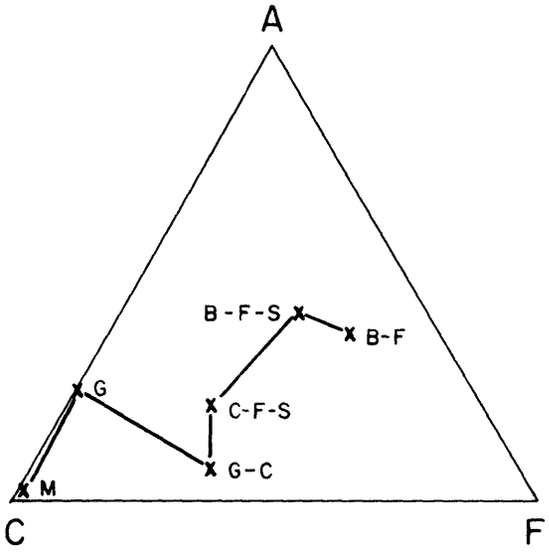

TRAVERSE 371-1A

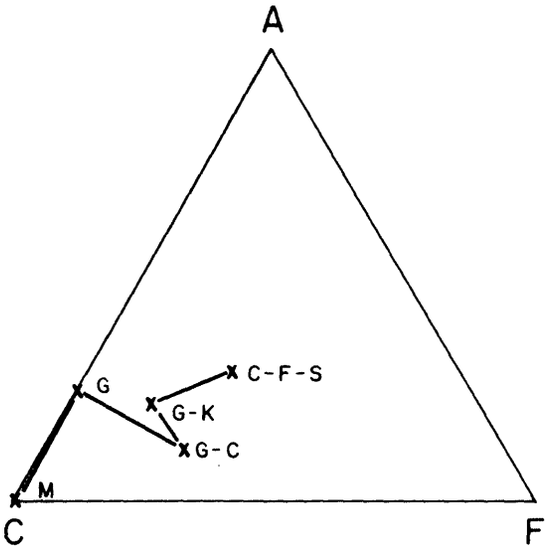

TRAVERSE 371-VS2

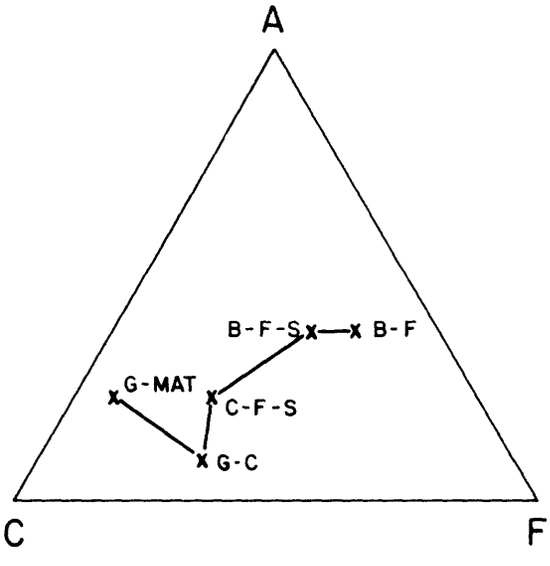

TRAVERSE 371-1B

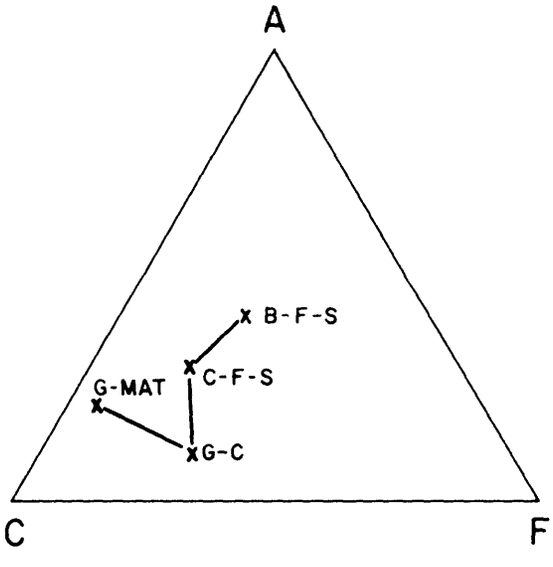

TRAVERSE 371-VI

compositions do not fall on a straight line between ACF plots of the end-member compositions, and therefore do not appear to represent simple mixtures of these end members. These departures from linearity require changes in the relative proportions of Al_2O_3 ($+Fe_2O_3$) and MgO (+FeO) in different parts of the reaction bands. Using traverse 371-1A (Fig. 5-4A) as an example, the major deviations from a simple trend between the biotite + feldspar unit and the marble involve the garnet + clinopyroxene and garnet layers. The garnet + clinopyroxene layer requires a distinct enrichment in F relative to A, and conversely the monominerallic garnet layer contains no F component, plotting on the C-A side of the ACF triangle. This marked variation from a simple compositional trend on an ACF diagram was also noted by Thompson (1975a) in his description of a reaction band between marble and pelite.

Assemblages defined in an ACF diagram by a continuous change in composition between plots of the original rock types (i.e. three-phase assemblages separated by two-phase boundaries) do not represent the changes in mineralogy across a reaction band. This has been discussed by Brady (1977, pp.114-115), and is evident from the mineral assemblages and the discontinuous variation in molar composition across the reaction bands in this study. The discontinuous changes in composition are believed to be characteristic of diffusion because diffusion can cause continuous changes in chemical potential to exist across the layers without causing continuous changes in the molar compositions. This concept has been outlined by Korzhinskii (1959), and discussed by Thompson (1959,1970). It will be described further in the genesis of the reaction bands in Section 5.9.

5.7 MASS BALANCE CALCULATIONS

5.7.1 Introduction

The reaction bands are believed to have developed by the redistribution (diffusion) of chemical components between originally juxtaposed chemically incompatible lithologies (e.g. marble and pelite). From the present distribution of components across the reaction bands, as outlined in Section 5.6), mass balance calculations can be made to examine this hypothesis. A knowledge of the originally juxtaposed rock compositions, the position of the initial boundary in the reaction band, the volume

change that has taken place, and the overall gain or loss of components from the system are required to allow mass balance calculations to be made. As these requirements cannot be unequivocally determined in this work, the calculations are made on the basis of certain assumptions. The validity of these assumptions can then be evaluated from the results obtained.

In this section mass balance calculations are made for traverse 371-1A (marble → pelite reaction band). These calculations are made assuming constant volume and no overall gain or loss of components from the system. The biotite + feldspar unit and marble are used as the originally juxtaposed rock types, and it is inferred from petrographic evidence (Section 5.4) that the initial boundary occurs between the felsic layer and the clinopyroxene + garnet layer. Calculations are based on layer compositions presented in Table 5.4, and the results are shown in Table 5.5. These results are obtained by subtracting the number of moles per 100 cm^3 in the original rock from that of the layer assumed to have replaced it, multiplied by the thickness (in $\frac{1}{100}$ mm) of the layer concerned (i.e. for convenience it is taken that the 100 cm^3 volume represents an area of 100 cm x 100 cm by a thickness of $\frac{1}{100}$ cm across the reaction band). Hence, a negative sign represents the number of moles liberated by the conversion, whereas a positive sign signifies the number of moles gained.

TiO_2 has not been considered in these calculations because the sphene-rich rim at the proposed initial boundary has not been considered in the compositions of Table 5.4, and because of the uncertainty associated with the increase in Ti from the biotite + feldspar unit to the sphene-bearing layers (Section 5.6). It should be emphasised that results of this type can aim to be no more than tenuous, considering the uncertainties in the figures used. These include variations in modal content (and the difficulties in point counting such fine-grained material), the variable thickness of the layers, and most significantly, variations in mineral chemistry within the layers.

5.7.2 Results and Discussion

From the results in Table 5.5 it can be seen that mass balance, although not achieved for all oxides, is extremely close for Al_2O_3 and MgO (remarkably so considering the uncertainties in these calculations). This gives some credibility to the assumptions made earlier (Section 5.7.1).

TABLE 5.5. Mass-balance calculations of oxide components across the marble→pelite reaction band - traverse 371-1A (based on constant volume)

371-1A	SiO_2	Al_2O_3	Fe_2O_3	FeO	MgO	CaO	Na_2O+K_2O
MARBLE → GT LAYER	+73.595	+19.275	+ 7.546	-	-	-10.371	
MARBLE → CPX+GT LAYER	+17.563	+ 1.907	+ 0.725	+ 1.880	+13.700	-14.165	
BI+FELD → FELSIC LAYER	+ 9.686	- 5.101	-	- 4.631	- 2.507	+ 5.220	+0.491
BI+FELD → CPX+FELD+SPH LAYER	+28.038	-13.812	-	-13.368	+ 0.366	+41.530	-8.400
BI+FELD → BI+FELD+SPH LAYER	+ 8.954	- 2.123	-	-13.662	-11.760	+11.022	+0.198
			+ 8.271	-29.781			
			ALL AS FeO				
			+16.542	-29.781			
SUM ACROSS THE REACTION BAND	+137.836	- 0.146		-13.239	- 0.201	+33.237	-7.711

Values calculated from the data of Table 5.4. These values represent the differences in moles of oxides per 100 cm^3 between the particular layer and the end-member lithology from which it is assumed to have been derived (indicated in the left-hand-side column), multiplied by the layer width (in 1/100ths of mm) given in Table 5.1.

-Ve sign refers to the number of moles liberated by the conversion indicated.
+Ve sign refers to the number of moles gained by the conversion indicated.

Abbreviations shown in Table 5.2A.

Relocating the initial boundary causes imbalance in these two oxides (as well as exaggerating the overall imbalance of the others). It is also concluded from Table 5.5 that the Al_2O_3 required in the formation of the garnet and garnet + clinopyroxene layers has been derived primarily from the conversion of biotite to clinopyroxene. Similarly the MgO now present in the garnet + clinopyroxene layer appears to have been derived from the formation of the biotite + feldspar + sphene and felsic layers.

There is a significant deficiency in the number of moles of CaO required to form the fine-grained calc-silicate layers (on the non-carbonate side of the proposed initial boundary) compared to that released from the formation of the garnet and garnet + clinopyroxene layers. This could imply a decrease in volume of the original marble, as expected in the conversion of a carbonate to a denser assemblage of garnet and clinopyroxene. The required decrease in thickness across the reaction band equivalent to this volume decrease is 0.134 mm, which is feasible. The major discrepancy in the mass balance calculations is in SiO_2. In traverse 371-1A, all layers in the reaction band require more SiO_2 than present within an equivalent volume of biotite + feldspar unit. Therefore, assuming constant volume, it is not possible to derive these layers from the biotite + feldspar unit without a major addition of SiO_2 to the system. A volume decrease associated with the conversion of the biotite + feldspar unit to these layers could explain this imbalance. This would have required a decrease of 0.65 mm in the thickness of the biotite + feldspar unit to form the fine-grained layers on the non-carbonate side of the initial contact (these layers represent a total thickness of 1.88 mm in the reaction band). Although some volume decrease is likely because of the loss of H_2O associated with the formation of the non-hydrous calc-silicate phases, such a relatively major decrease in volume would cause large imbalances in both MgO and Al_2O_3 (as well as in FeO and the alkalis). Therefore, it is more likely that the original non-carbonate rock had higher SiO_2 values than the biotite + feldspar unit. This was probably pelite, and the biotite + feldspar unit is believed to have been derived from the pelite by addition of CaO and loss of SiO_2 (more fully described in Section 5.8). This would readily explain the unusual quartz-free assemblage of this rock unit.

Excess FeO and alkalis appear to result from the formation of the

reaction band (Table 5.5). FeO is mainly released by the formation of the biotite + feldspar + sphene and the clinopyroxene + feldspar + sphene layers. Some of the FeO is balanced by the Fe_2O_3 in the garnet, with the Fe seemingly changing its oxidation state, but FeO still remains in excess. K_2O is derived mainly from the formation of clinopyroxene in preference to biotite. Although some K_2O is accounted for by the enrichment of K-feldspar in the felsic layer and amongst the thin concentration of sphene at the felsic : garnet + clinopyroxene layer boundary (not recorded), this is insufficient to balance the K_2O released from the breakdown of biotite. Two possibilities are suggested for the excess of FeO and K_2O. Firstly, lenses rich in Cu-Fe sulphides and feldspar (predominantly K-feldspar) occur throughout the fine-grained layers (Section 5.4). These lenses also have K-feldspar-rich rims, and since neither the lenses nor the rims have been included in the modes used in the mass-balance calculations, they could explain the apparent excess shown in the results. Secondly, it is possible that the FeO and K_2O are simply lost from the rocks via aqueous solutions.

5.7.3 Summary and Conclusions

These results support the hypothesis that reaction bands form by chemical redistribution across the contact between chemically incompatible lithologies. Location of the initial contact between the felsic and garnet + clinopyroxene layers on the basis of textural evidence is consistent with the mass-balance calculations, especially for MgO and Al_2O_3.

It appears that the garnet and garnet + clinopyroxene layers have been derived from marble by the addition of SiO_2, Al_2O_3, MgO, FeO and Fe_2O_3. Al_2O_3 was derived primarily by the conversion of biotite to clinopyroxene. MgO and FeO were derived by formation of the biotite + feldspar + sphene and felsic layers, with FeO also released by the formation of clinopyroxene in the clinopyroxene + feldspar + sphene layer. Some FeO was apparently oxidised to Fe_2O_3 and substituted for Al_2O_3 in the garnets. SiO_2 was derived presumably by the formation of the feldspar-bearing layers, including the biotite + feldspar unit, from original pelite. The formation of the garnet and garnet + clinopyroxene layers from marble has released CaO which was used in the conversion of the original pelite to a sequence of calc-silicate layers. This has resulted in a stepwise decrease in CaO content of the layers away from the marble. Therefore, there appears to

have been a simultaneous reciprocal exchange of chemical components across the original contact. However, K_2O and TiO_2 do not occur on the marble side of the original contact. The redistribution of chemical components across the reaction bands is considered in more detail in Section 5.9.

A decrease in the volume of the original marble seems necessary to balance the CaO required in the conversion of the original non-carbonate material of the reaction band. Conversely, although some decrease in volume is possible, a major decrease in the volume of the original non-carbonate side of the reaction band does not seem necessary, assuming that the deficiency in SiO_2 can be explained by the biotite + feldspar unit being poorer in SiO_2 than the original non-carbonate rock (taken here to be pelite).

Although the chemical components can be broadly balanced without major addition or removal of components from the system (excluding volatiles), it is possible that some FeO and K_2O was lost during formation of the reaction band.

5.8 REACTIONS

By using the mineral analyses and modal data, equations can be written expressing the formation of the layers from the original rock. These equations show the excess oxides required or released by the reactions, and consequently restate the results of the mass-balance calculations.

5.8.1 Biotite + Feldspar Unit

It has been inferred from the mass-balance calculations and the simple mineralogy of the unit that it has been derived from a previous quartz-bearing rock by addition of CaO. From the fine-grained texture of the biotite + feldspar unit and its composition, it is most likely that it was originally a pelitic sediment. A typical pelitic assemblage at the metamorphic conditions suggested (Section 5.3) is biotite + quartz + K-feldspar + plagioclase (? An 20-30) + Al-bearing silicate. Although the Al-bearing silicate is most likely to be cordierite (an extremely weathered exposure of cordierite hornfels, containing biotite + quartz + K-feldspar + plagioclase + cordierite, occurs adjacent to the impure calcirudites in the costean at sample locality 371), for convenience of

illustration the Al-bearing silicate is assumed here to be an Al_2SiO_5 polymorph. With the addition of CaO to this assemblage, a reaction involving the breakdown of the Al-silicate is suggested:

$$CaO + Al_2SiO_5 + SiO_2 \rightarrow CaAl_2Si_2O_8$$

This reaction appears to exhaust the Al-silicate, deriving the biotite + K-feldspar + plagioclase (An 90) assemblage of the biotite + feldspar unit, with excess SiO_2 assumedly diffusing toward the marble.

Reactions for the formation of the biotite + feldspar + sphene and clinopyroxene + feldspar + sphene layers are based on data using the biotite + feldspar unit as the original rock type. Therefore it should be remembered that the original pelitic material would be richer in SiO_2 and slightly poorer in CaO than the composition of the biotite + feldspar unit.

5.8.2 Biotite + Feldspar + Sphene Layer

Based on the modal data of traverse 371-1A (Table 5.6, taken from Table 5.1 and converted to moles per 100 cm^3), the general reaction involves the breakdown of the red-brown biotite to form a pale-brown biotite (poorer in Ti) plus K-feldspar and sphene, with the plagioclase content remaining relatively constant. From these modal data and the mineral analyses of Table 5.2A, reaction 5-I is derived:

$$1.00\ \text{Biotite(1)} + 0.20\ CaO + 0.48\ SiO_2 \rightarrow 0.69\ \text{Biotite(2)} + 0.63\ \text{K-feldspar} + 0.20\ \text{Sphene} + 0.62\ H_2O + 0.65\ MgO + 0.75\ FeO + 0.20\ Al_2O_3 \qquad 5\text{-I}$$

REACTANTS

Biotite(1) $K_{2.0}Al_{.81}Ti_{.28}Fe_{1.98}Mg_{2.62}Si_{5.2}Al_{2.8}O_{20}(OH)_4$

PRODUCTS

Biotite(2) $K_{2.0}Al_{.93}Ti_{.17}Fe_{1.79}Mg_{2.86}Si_{5.2}Al_{2.8}O_{20}(OH)_4$

Sphene $Ca_{1.0}Ti_{.9}Al_{.1}Si_{1.0}O_5$

The SiO_2 in the reactants represents the extra quartz believed to be present in the pelitic rock compared to the biotite + feldspar unit. Less sphene is formed in the products of reaction 5-I than predicted from the modal data in Table 5.6 (a coefficient for sphene of 0.66 would be required

TABLE 5.6. Conversion of modal per cent to moles per 100 cm^3 for part of traverse 371-1A

		BIOTITE	K-FELDSPAR	PLAGIOCLASE	SPHENE	CLINOPYROXENE
BI+FELD UNIT						
	MODAL %	*49.84	14.56	35.60		
	MOLES	0.1636	0.1363	0.3536		
BI+FELD+SPH	LAYER					
	MODAL %	**34.18	26.55	33.29	5.98	
	MOLES	0.1124	0.2485	0.3306	0.1075	
CPX+FELD+SPH	LAYER					
	MODAL %		21.11	33.44	7.95	37.50
	MOLES		0.1976	0.3321	0.1429	0.5592

* Red-brown biotite

** Pale-brown biotite

Abbreviations shown in Tables 5-2A→E.

to be consistent with the modal data). This reflects the apparently low Ti content of the biotite + feldspar unit compared to the biotite + feldspar + sphene layer, noted in Fig. 5-2A.

5.8.3 Clinopyroxene + Feldspar + Sphene Layer

Again using the modal data of Table 5.6 and the mineral data of Table 5.2A, a reaction for the formation of clinopyroxene from biotite consistent with the mass balance calculations is given as

$$1.00 \text{ Biotite} + 3.68 \text{ CaO} + 2.95 \text{ SiO}_2 \rightarrow 3.36 \text{ Clinopyroxene} + 0.37 \text{ K-feldspar} + 0.16 \text{ Sphene} + 2.00 \text{ H}_2\text{O} + 1.38 \text{ FeO} + 1.61 \text{ Al}_2\text{O}_3 + 0.82 \text{ K}_2\text{O} \qquad \text{5-II}$$

REACTANTS

Biotite $K_{2.0}Al_{.81}Ti_{.28}Fe_{1.98}Mg_{2.62}Si_{5.2}Al_{2.8}O_{20}(OH)_4$

PRODUCTS

Clinopyroxene $Ca_{1.0}Fe_{.18}Mg_{.78}Si_2O_6$

Sphene $Ca_{1.0}Ti_{.9}Al_{.1}Si_1O_5$

The comments made with reference to quartz and sphene in association with reaction 5-I are also relevant to reaction 5-II.

5.8.4 Further Discussion

Formation of the felsic layer is basically represented by equation 5-II, except that the amount of clinopyroxene formed is decreased, and the amount of K-feldspar and sphene increased. The formation of the garnet and garnet + clinopyroxene layers are simply envisaged as $CaCO_3$ reacting with SiO_2, Al_2O_3, and MgO that have diffused into the marble from the adjacent pelite. The lack of calcite and quartz in these layers from excess CaO and SiO_2 suggests that these chemical components have been free to move throughout these layers (discussed fully in Section 5.9).

5.9 PETROGENESIS OF THE REACTION BANDS

5.9.1 Introduction and Review

Several authors (referred to in the introduction to this chapter) have discussed the petrogenesis of layers produced between Ca-rich and

Ca-poor rock types, and have developed concepts (and associated terminology) necessary to the understanding of diffusion. Three concepts that have proved to be repeatedly useful are those of local equilibrium, chemical potential gradients (as distinct from differences in bulk-rock composition), and the internal and external control of chemical potentials of the components. These concepts will now be briefly outlined, with reference to more detailed discussions in other works.

The concept of local equilibrium states that although a large volume of rock may be out of equilibrium, any part of that system can be taken to be in equilibrium if made small enough (Thompson, 1959). Each point across a reaction band can therefore be considered to be in local equilibrium (Brady, 1977). Chemical potential gradients established across the reaction band are the driving force for diffusion. Diffusion occurs to reduce these chemical potential gradients, so that with time (during metamorphism) discontinuities are eliminated and the chemical potentials of the diffusing components will vary monotonically and continuously across the reaction bands (Brady, 1977). Therefore, although discontinuous breaks occur in bulk composition across the reaction bands, chemical potentials are continuous. This was recognised by Thompson (1959), and has been discussed more fully by Joesten (1974, pp.893-894). The concept is shown diagramatically by Ildefonse and Gabis (1976, Fig. 4, where concentration in the pore fluid is equivalent to chemical potential in the pore fluid).

Thirdly, the concept of components having their chemical potentials controlled outside a chosen local equilibrium is described by Korzhinskii (1959, Chapter IV), and Thompson (1970). In summary, if the chemical potential of a diffusing component is controlled by the diffusing process (i.e. its position in the continuous potential gradient) rather than the local equilibrium assemblage, then with regard to that assemblage the chemical potential of that component is externally controlled. In this study, such components will be referred to as K-components whereas components whose chemical potentials are locally controlled will be referred to as J-components. This terminology is that of Thompson (1970). In the discussion of diffusion, these terms are equivalent to the terms 'perfectly mobile' and 'inert' respectively, as used by Korzhinskii (1959), (though, as pointed out by Thompson, 1970, pp.543-544, the terms 'K-component' and 'perfectly mobile' are distinct because K-components also include what

Korzhinskii would have defined as "excess" components). Vidale and Hewitt (1973) used the terms 'inert' and 'mobile', but these terms will be avoided here because of the connotations attached to them that need not apply (Thompson, 1970). It is noteworthy that both K- and J-components can be diffusing components (Joesten, 1974; Brady, 1977) with 'diffusing components' referrring, in the sense of Brady (1977), to any components which have moved relative to inert (stationary) markers.

In terms of the phase rule Thompson (1959, pp.453-455; 1970, pp.541-545), and Vidale and Hewitt (1973) have shown that the maximum number of phases possible within a given layer is decreased by an amount equivalent to the number of K-components. That is, $F = C-P+2-m$ where F = degrees of freedom (equal to two, for temperature and pressure), C = total number of components, P = number of phases, m = number of K-components. As discussed by Thompson (1970), this is not a "modified" phase rule, but a consequence of the Gibb's phase rule, where the number of independently chosen variables (variance) is $F(2)+m$.

Chemical potential diagrams, as introduced into the literature by Korzhinskii (1959, and many earlier publications), and described by Burt (1974), are used to schematically represent solid phases that occur in local equilibrium with an associated intergranular pore fluid. The solid phases vary with changes in the chemical potentials of the components free to diffuse within the fluid (i.e. diffusing components). These diagrams (for three components) define a saturation surface, whose faces represent the locus of chemical potential values (for the components considered) for which a solid phase (or several phases) coexist in equilibrium with the fluid (Joesten, 1977, p.651). Should the locus of chemical potentials lie inside this surface, the fluid is undersaturated in the components with respect to the solids and no phase is precipitated (Joesten, 1977; Burt, 1974). Chemical potential diagrams can only conveniently deal with three diffusing components (though Grant (1977) has attempted to display four components by use of crystallographic projection).

The term 'flux' will be used in the following discussion as a measure for the relative transport of the components. Flux is the rate of transfer of a component through a unit area of a section, and from Fick's first law, flux is proportional to the concentration gradient normal to that section (Frantz and Mao, 1976, p.280). This can be alternatively expressed

as flux being equal to the diffusion coefficient multiplied by the concentration gradient (Ildefonse and Gabis, 1976). The diffusion coefficient refers to the velocity at which components move through an intergranular fluid, while the concentration gradient of the components in the pore fluid is equivalent to the chemical potential gradient in the pore fluid. The concentration gradient depends on the chemical differences between the local assemblages and the solubility of the components in the fluid medium. Flux is also dependent on the properties of porosity and tortuosity within the rocks (Frantz and Mao, 1976). However, when considering the relative movement of components within a given reaction band, these properties are constant for all components and need not be considered.

The diffusing components and their chemical potentials are referred to below in terms of oxides. This is consistent with recent papers (e.g. Joesten, 1977; Brady, 1977; Sanford, 1980). However this practice is used here merely as a means of notation, and implies nothing about the state in which the chemical components have moved in the pore fluid.

5.9.2 Formation of the Marble → Pelite Reaction Bands

The following discussion aims to outline the formation of the marble → pelite reaction bands described in the previous sections (e.g. Traverse 371-1A) in terms of the above concepts. These reaction bands have all been sampled from the same locality (sample locality 371), which has prevented investigation of their development with increasing temperature. Therefore, it is assumed that the layers have developed simultaneously at the onset of diffusion. The simultaneous development of layers has been shown experimentally by Ildefonse and Gabis (1976). Modification with temperature and time, especially widening of the zones (Brock, 1972; Thompson, 1975a) is not denied; nevertheless, this does not affect the conclusions drawn here.

The general sequence of layers is

marble
garnet
garnet + clinopyroxene
felsic (K-feldspar + sphene ± clinopyroxene ± plagioclase)
clinopyroxene + feldspar + sphene
biotite + feldspar + sphene
biotite + feldspar unit

Figure 5-4: ACF diagrams of bulk composition across the reaction bands

$A = Al_2O_3 + Fe_2O_3$

$C = CaO$

$F = FeO + MgO$

The plots are calculated from the data of Table 5.4.

The lines between the plots link the individual compositions in sequence across the reaction bands.

Abbreviations: B-F = biotite + feldspar unit, B-F-S = biotite + feldspar + sphene layer, C-F-S = clinopyroxene + feldspar + sphene layer, G-K = garnet + K-feldspar layer, G-C = garnet + clinopyroxene layer, G = garnet layer, M = marble, G-MAT = garnet-rich matrix.

with the garnet + clinopyroxene : felsic layer boundary marking the original contact between marble and pelite (Sections 5.4 and 5.7). From the mass balance calculations of Section 5.7 it is most likely that the biotite + feldspar unit is also a Ca-enriched layer, with the pelite originally containing quartz. Formation of the felsic layer is not considered here, because of its variable characteristics (Sections 5.4 and 5.6), but two possibilities for its origin are briefly discussed in Section 5.9.5. Owing to the absence of consistent systematic changes in mineral chemistry across the layers (Section 5.5), the solid solution pairs Al_2O_3-Fe_2O_3, MgO-FeO, and K_2O-Na_2O are considered as single components Al_2O_3, MgO, and K_2O respectively. The layers will be discussed in order across the reaction band, beginning with the monomineralic garnet layer.

Garnet Layer

Formation of the garnet layer has required introduction of SiO_2, Al_2O_3 into the marble and loss of CaO (Section 5.7). Therefore, all components were diffusing components. No obvious change in bulk chemistry occurs across the layer (garnet composition remains relatively constant, Section 5.5). However, chemical potential gradients existed across the layer, and these were responsible for the diffusion of the components. If time (the period of metamorphism) was sufficient (as can be assumed), the chemical potentials of the diffusing components would have varied smoothly and continuously across this layer. This is depicted on the chemical potential diagram of Fig. 5-5 (and the μCaO-μSiO_2 projection, Fig. 5-5A). Garnet in equilibrium with the pore fluid is represented by the oblique face on the saturation surface. The arrow represents the schematic changes in chemical potentials in the pore fluid across the garnet layer. As the marble is approached the chemical potentials of SiO_2 and $AlO_{3/2}$ decrease, while the chemical potential of CaO increases. Eventually a situation is reached (which depends on the ratios between the three components) where calcite is the stable phase in equilibrium with the pore fluid, not garnet. This marks the end of the garnet zone, and a sharp change in bulk chemistry of the solid phases, though denoting only a small change in the chemical potentials of the components across the actual boundary.

Although all three components were diffusing, and therefore had chemical potentials which varied systematically across the layer, at any point of local equilibrium within the layer, the components in solution

Figure 5-5: Schematic chemical potential diagram for SiO_2-CaO-$AlO_{3/2}$ (plus the μSiO_2-μCaO projection, Fig. 5-5A).

The faces form part of the saturation surface and represent solid phases in equilibrium with the diffusing components in the pore fluid. The arrow represents the change in chemical potentials of the diffusing components in the pore fluid across the garnet layer (this also applies to the μSiO_2-μCaO projection).

WOLL = wollastonite

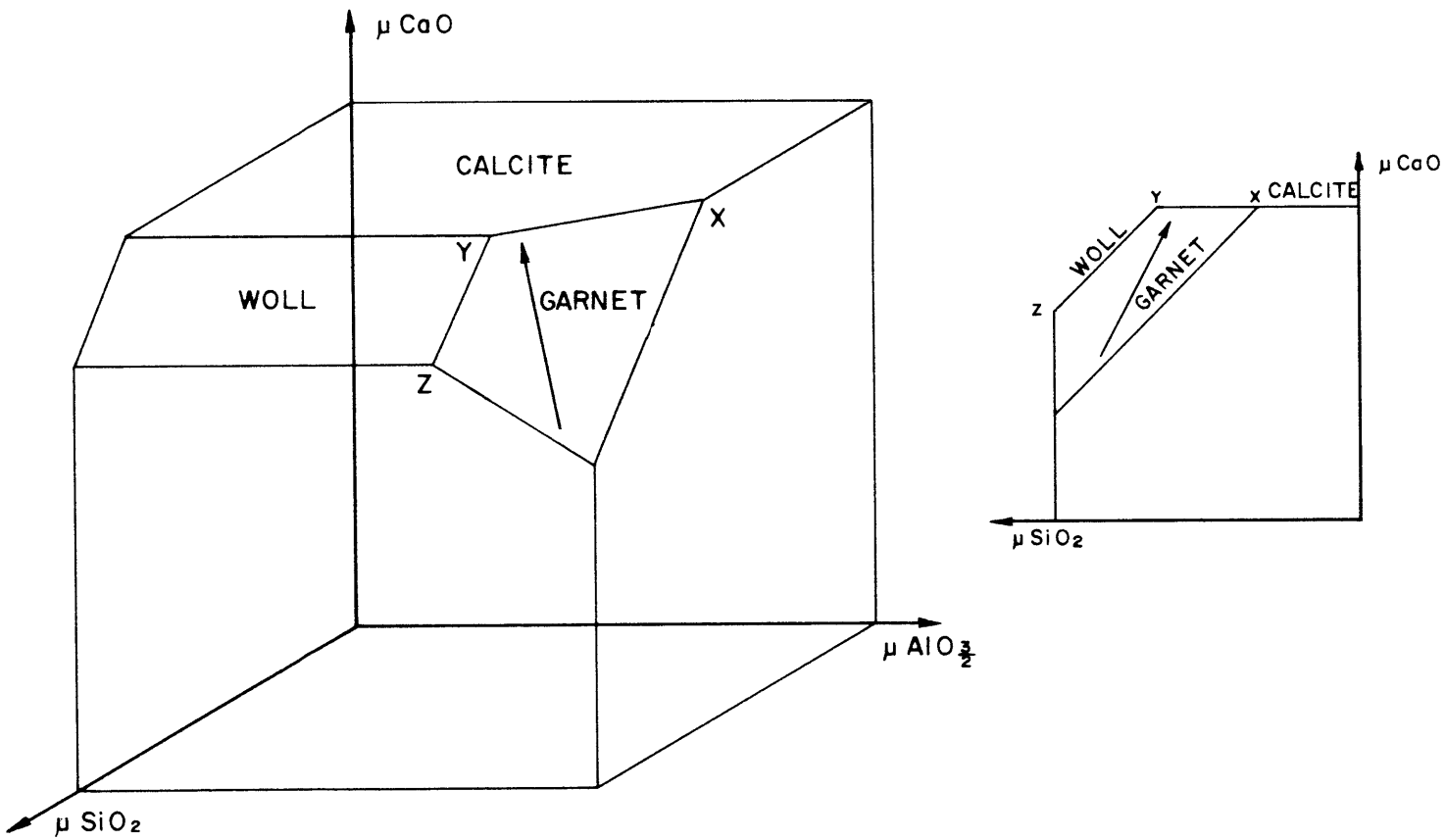
μ CaO
CALCITE
X
Y
WOLL
GARNET
Z
μ AlO 3/2
μ SiO2
μ CaO
Y
X CALCITE
WOLL
GARNET
Z
μ SiO2

were in equilibrium with the single phase, namely garnet. Consequently, as noted by Joesten (1974, p.897) and Brady (1977, p.119), only two of these components (n-1, being the number of components) can have their chemical potentials randomly defined (chosen external to the local system), with the third being defined by the presence of the garnet. This can also be seen from the chemical potential diagram (Fig. 5-5); for if the chemical potentials of any two components are randomly chosen, and the locus of chemical potentials must be consistent with the presence of garnet (i.e. lie in the plane defining garnet), then the chemical potential of the third component is fixed. But, this does not fix the chemical potential of the third component throughout the layer. On the contrary, as the two randomly chosen components vary across the layer, so must the third to maintain local equilibrium between the pore fluid and the garnet.

Therefore, within the garnet layer only two of the components can be considered as K-components (having chemical potentials controlled outside the local equilibrium), and the third must be taken as a J-component. In terms of the phase rule, for a given temperature and pressure, one phase (garnet) has formed from three components, two of which are K-components. That is, $F(2) = C(3) - P(1) + 2 - m(2)$. To specifically designate one of the components as a J-component would be misleading. This is because the fact that only two of the three components can be considered to be K-components does not imply anything specific about any one of the components, but rather that the presence of one phase reduces by one the number of variables that can be independently chosen.

Garnet + Clinopyroxene Layer

In the garnet + clinopyroxene layer an extra component is involved, with MgO as well as Al_2O_3 and SiO_2 having diffused into the original marble, in association with the loss of CaO into the pelite. Hence, all components were diffusing components, and chemical potential gradients existed across the layer even though its composition was relatively uniform. Difficulties occur in representing the four diffusing components on a chemical potential diagram. However, neither of the phases need be expressed in terms of all four components. Garnet involves only the components CaO, SiO_2 and Al_2O_3, and clinopyroxene CaO, SiO_2 and MgO. Therefore, a chemical potential diagram can be constructed by superimposing two chemical potential diagrams involving these components. The resultant

diagram (Fig. 5-6) has axes representing CaO and SiO_2, and a common third axis representing the mutually exclusive components $AlO_{3/2}$ and MgO.

The arrow in Fig. 5-6 represents the schematic changes in chemical potentials of the components in the pore fluid across the garnet + clinopyroxene and garnet layers (N.B. for ease of representation only one arrow is shown, though strictly this implies that the chemical potentials of $AlO_{3/2}$ and MgO are equal, which is most unlikely). The μSiO_2-μCaO projection of Fig. 5-6 is also shown (Fig. 5-6A) and the arrow depicted on this projection is equivalent to that shown in Fig. 5-6. The base of the arrow represents part of the garnet + clinopyroxene layer, with clinopyroxene stable in the CaO-SiO_2-MgO system and garnet stable in the CaO-SiO_2-$AlO_{3/2}$ system. In the μSiO_2-μCaO projection this situation exists above both lines A-B and C-D. Across the layer the chemical potential of CaO increases, whereas the chemical potentials SiO_2, $AlO_{3/2}$, and MgO decrease. This continues until clinopyroxene is no longer in equilibrium with the pore solution (i.e. the arrow in Fig. 5-6A crosses line C-D), which marks the limit of the clinopyroxene + garnet layer. However, garnet continues to be in equilibrium with the pore solution in the garnet layer as described above. With reference to the phase rule, although all four components are diffusing, because of the presence of two phases, only two components can be considered as K-components (each phase restricting the number of independently chosen variables by one); that is,

$$F(2) = C(4) - P(2) + 2 - m(2).$$

Layers on the Pelite Side of the Original Boundary

Layers on the pelite side of the original boundary are complicated by the presence of a greater number of initial components. $KO_{\frac{1}{2}}$ and TiO_2 do not occur on the marble side of the original boundary (traverse 371-VS2 a possible exception) and can be considered to have been non-diffusing components in these reaction bands. They were J-components. All other components, SiO_2, CaO, $AlO_{3/2}$, MgO, were diffusing components.

The clinopyroxene + feldspar + sphene layer represents an assemblage in equilibrium with both the diffusing and non-diffusing components. The chemical potentials of the diffusing components varied across the layers, whereas those of the non-diffusing components remained constant. The solid phases in equilibrium with the diffusing components of the pore fluid

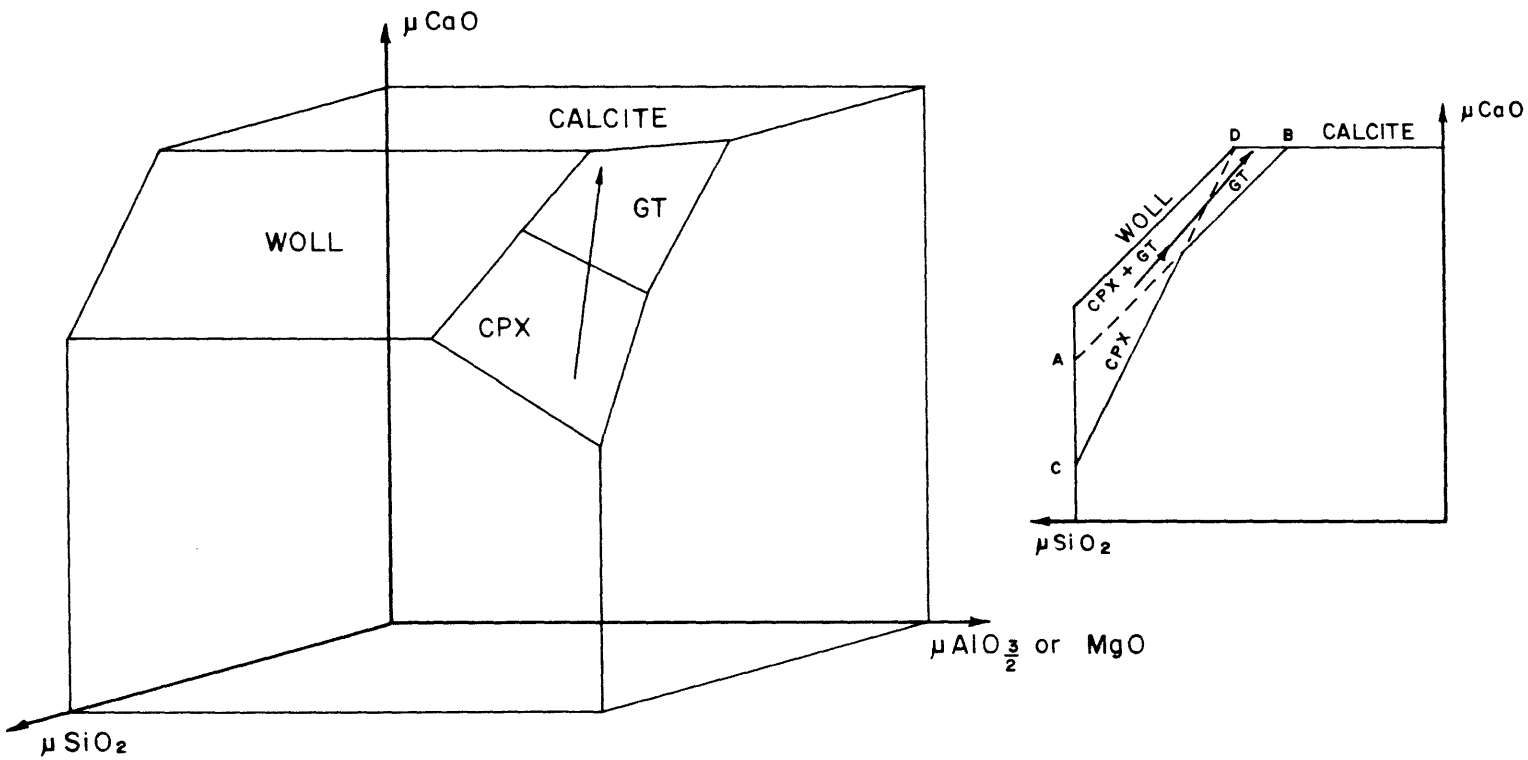
μCaO
CALCITE
WOLL
GT
CPX
μSiO2
μAlO3/2 or MgO
μCaO
D
B
CALCITE
WOLL
GT
CPX + GT
CPX
A
C
μSiO2

Figure 5-6: Schematically superimposed chemical potential diagrams for the systems SiO_2-CaO-$AlO_{3/2}$ and SiO_2-CaO-MgO (plus the μSiO_2-μCaO projection, Fig. 5-6A).

The faces form part of the saturation surface and represent solid phases in equilibrium with the diffusing components in the pore fluid. The join between the clinopyroxene and garnet faces of the saturation surface is only applicable if $\mu MgO = \mu Al_2O_3$. The arrow represents the change in chemical potentials of the diffusing components in the pore fluid across the garnet and garnet + clinopyroxene layers (this also applies to the μSiO_2-μCaO projection) (see text).

CPX = clinopyroxene, GT = garnet,
WOLL = wollastonite

in this layer were clinopyroxene and anorthite. Clinopyroxene was stable with regard to the diffusing components SiO_2, CaO and MgO, as in the garnet + clinopyroxene layer. However, anorthite was stable in preference to garnet in the $CaO\text{-}SiO_2\text{-}AlO_{3/2}$ system, associated with an increase in the chemical potentials of SiO_2 and $AlO_{3/2}$, and a decrease in the chemical potential of CaO. This is schematically shown on the μSiO_2-μCaO projection in Fig. 5-7. Anorthite is stable below line A-B', and the arrow represents the progression from the clinopyroxene + feldspar + sphene layer across the reaction band to the marble. Two further phases were defined in the clinopyroxene + feldspar + sphene layer by the presence of the non-diffusing J-components $KO_{\frac{1}{2}}$ and TiO_2. These were K-feldspar and sphene respectively. Therefore, this layer involves six components in four phases and, as in the garnet + clinopyroxene layer, only two of the four diffusing components can be considered to be K-components, the other two being locally defined by the presence of clinopyroxene and anorthite. That is,

$$F(2) = C(6) - P(4) + 2 - m(2).$$

A similar argument applies to the six component, four phase, biotite + feldspar + sphene layer. However, with further decreases in the chemical potential of CaO and increases in the chemical potentials of SiO_2, MgO and $AlO_{3/2}$, biotite was stable in preference to clinopyroxene as the ferromagnesian phase in equilibrium with the pore fluid. Anorthite remained stable in the $CaO\text{-}SiO_2\text{-}AlO_{3/2}$ system, and $KO_{\frac{1}{2}}$ and TiO_2 continued to define the K-feldspar and sphene.

The biotite + feldspar unit, taken as a slightly Ca-enriched layer, can also be discussed in this manner. However, with the loss of sphene, due to the decreasing chemical potential of Ca, no phase appears to be defined by TiO_2. This may support the presence of a further Ti-bearing phase (not identified) in the biotite + feldspar unit, as suggested in Section 5.6.

Summary and Discussion

Fig. 5-8 is a schematic representation of the layers formed across the marble → pelite reaction bands in relation to the changing chemical potentials of the components in the pore fluid. The actual gradients in chemical potential are not known, and intersections between the curves are purely diagrammatic. Fig. 5-8 is a summary of the above discussion.

Figure 5-7: Schematically superimposed μSiO_2-CaO projections for the systems SiO_2-CaO-$AlO_{3/2}$ and SiO_2-CaO-MgO. The arrow represents the change in chemical potentials of the diffusing components in the pore fluid across the clinopyroxene + feldspar + sphene, garnet + clinopyroxene, and garnet layers.

AN = anorthite, CPX = clinopyroxene, GT = garnet, WOLL = wollastonite

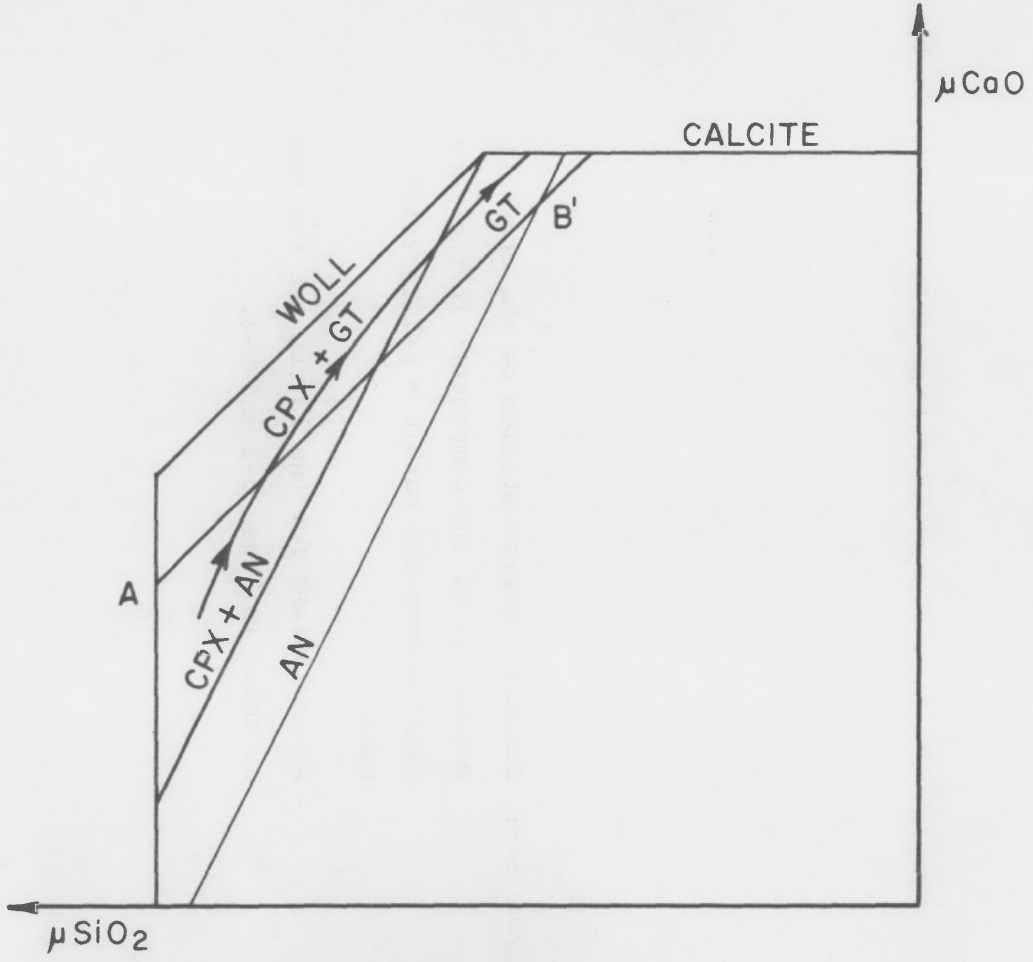
μCaO
CALCITE
B'
GT
WOLL
CPX + GT
A
CPX + AN
AN
μSiO2

Figure 5-8: Schematic representation of the chemical potentials of the components in the pore fluid across the marble → pelite reaction band.

Abbreviations for the layers are the same as those in Figs. 5-3 and 5-4.

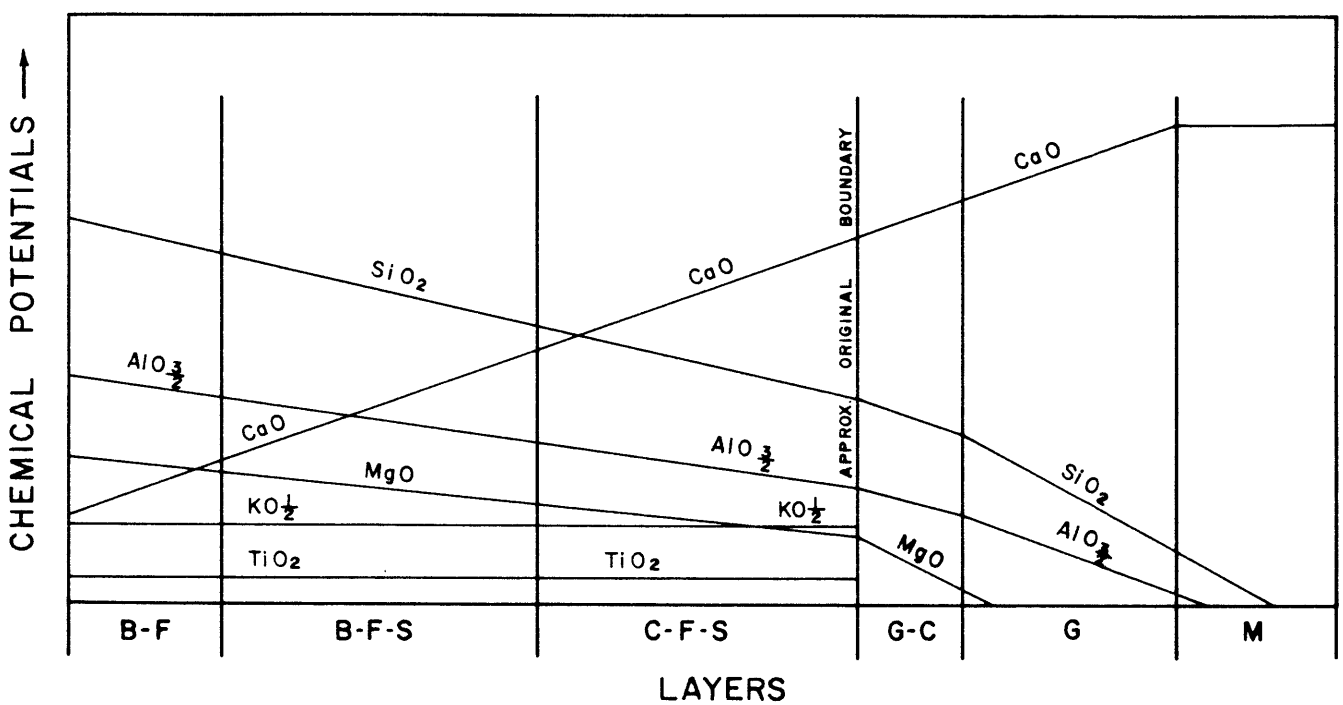
CHEMICAL POTENTIALS →
SiO2
CaO
AlO3/2
CaO
MgO
KO1/2
TiO2
APPROX. ORIGINAL BOUNDARY
CaO
AlO3/2
KO1/2
TiO2
MgO
SiO2
AlO3/2
B-F
B-F-S
C-F-S
G-C
G
M
LAYERS

The lack of wollastonite formation in these reaction bands is worthy of comment. It is best understood with reference to Fig. 5-5, where it is clear that wollastonite is not a stable phase because the $\mu AlO_{3/2}/\mu SiO_2$ ratio remains too high. The garnet layer ends with the arrow representing the changes in chemical potentials intersecting line X-Y rather than Y-Z. In reaction bands where the $\mu AlO_{3/2}/\mu SiO_2$ ratio is decreased slightly, the garnet layer could be followed by a wollastonite layer before the marble. This layer sequence is found in other examples of the study area, as described in T77B in Section 5.10.

5.9.3 Relative Movement of the Components

The aim of this section is to discuss the relative movements of the components in terms of flux and distance moved.

Flux

A measure of flux can be taken from the number of moles of a component transported across the original boundary in the period of metamorphism. This can be interpreted from Fig. 5-2 and has been calculated for traverse 371-1A in Table 5.5. The flux of both CaO and SiO_2 has been large compared to either $AlO_{3/2}$ or MgO, and the flux of $AlO_{3/2}$ has been more extensive than that of MgO. SiO_2, $AlO_{3/2}$ and MgO have all moved in the opposite direction (toward the marble) to CaO. Movement of $KO_{\frac{1}{2}}$ and TiO_2 into the marble has been very limited.

Flux of a component, as described in Section 5.9.1, is related to the component's diffusion coefficient and its concentration gradient (chemical potential gradient in the pore fluid) (assuming that the diffusion of a component due to chemical potential gradients in other components is zero, and that the physical properties of a rock can be ignored when comparing components in the same reaction band; Frantz and Mao, 1976). The different fluxes of the components, and indeed the different distances of diffusion (see below), could be explained by their different diffusion coefficients (velocities of transport through the fluid medium). However, Ildefonse and Gabis (1976, p.299) and Brady (1977, p.118) commented that, at conditions of metamorphism, diffusion coefficients of non-volatile components are probably very similar, and it is unlikely that differences in the movement of components can be attributed to differences in their diffusion coefficients. Therefore, the relative transport of the components

seems to be related to differences in chemical potential gradients.

Concentrations in the pore fluid (and hence chemical potential gradients set up in the pore fluid between the originally incompatible rock types) depend on both the concentrations of the components in the solid assemblage and the relative solubilities of the components. The dependence of a component's flux on its solubility in solution has been suggested by several authors (e.g. Ildefonse and Gabis, 1976; Sanford, 1980). It is likely that differences in solubility are affecting the relative fluxes of the components in this study. However, it is noted here that the different fluxes can be directly related to chemical differences in the original rock types. That is, large differences occur in the CaO and SiO_2 contents of the marble and pelite, while molar values in the biotite + feldspar unit descend in the order SiO_2, $AlO_{3/2}$ and MgO (the original pelite is likely to have been higher still in SiO_2), consistent with their relative fluxes into the marble. Furthermore, clinopyroxene from layers on either side of the original boundary have very similar compositions (Section 5.5). This similarity suggests that fluxes of MgO and FeO into the marble occur in a ratio which reflects the MgO/MgO+FeO ratio of the original pelite. This in turn implies that the solubilities of MgO and FeO are similar, otherwise the pyroxene forming within the original marble (in the garnet + clinopyroxene layer) would be expected to differ in its Mg/Mg+Fe ratio, relative to that in the clinopyroxene + feldspar + sphene layer, in favour of the component (either MgO or FeO) with the greater solubility. This relationship between flux and original rock chemistry will be discussed further with reference to reaction bands showing a range of non-carbonate compositions, in Section 5.10.

Distances Moved

CaO has diffused relatively large distances into the pelite compared to the movement of SiO_2, $AlO_{3/2}$ and MgO into the marble. SiO_2 and $AlO_{3/2}$ appear to have moved a similar distance, to the garnet layer : marble boundary, whereas MgO appears to be restricted to the garnet + clinopyroxene layer. The distance over which a component diffuses seems to depend on the flux of the component, and the rate at which the component is taken out of solution by the solid phases in local equilibrium with it. It is also emphasised that the apparent distance to which a component has moved is determined by its concentration in solution (chemical potential) falling

below a value required to form a phase containing that component.

In marble → pelite reaction bands, although both SiO_2 and CaO have high fluxes across the original boundary, the SiO_2 moves a much smaller distance than CaO. This is because the formation of clinopyroxene and garnet sharply reduces the concentration of SiO_2 in the pore fluid, whereas solid phases in equilibrium with the pore fluid (e.g. clinopyroxene and sphene) remove CaO from solution in smaller amounts for a given volume of rock. Similarly, the relative distances moved by MgO, $AlO_{3/2}$ and SiO_2 into the marble are related to both effects. The low flux and the extensive removal of MgO across the garnet + clinopyroxene layer causes MgO to be exhausted before $AlO_{3/2}$ and SiO_2 (or at least diminished to concentrations below those required for formation of clinopyroxene). The garnet layer : marble boundary does not designate where, by coincidence, both $AlO_{3/2}$ and SiO_2 have become exhausted from solutions, but merely the point where the combination of component chemical potentials is no longer consistent with the formation of garnet, and, even though μSiO_2 may be higher than $\mu AlO_{3/2}$, the $\mu SiO_2/\mu AlO_{3/2}$ ratio is not sufficiently high to allow wollastonite formation (Fig. 5-5).

The apparent lack of $KO_{\frac{1}{2}}$ and TiO_2 diffusion may reflect their low solubilities in the pore fluid. Although K was found by Vidale (1969) to have a high solubility in H_2O compared to Ca, Mg and Al, the presence of CO_2 in the pore solution could vastly alter their relative solubilities. Sanford (1980, p.667) recognised the decrease in solubility of SiO_2 in CO_2-rich fluids compared to H_2O-rich fluids, and this could also apply to $KO_{\frac{1}{2}}$ and TiO_2. Alternatively, although $KO_{\frac{1}{2}}$ and TiO_2 are not components in the phases formed within the original marble, it is possible that some diffusion of these components has occurred across the original boundary. However, their chemical potentials have not been sufficiently high to form phases containing them.

5.9.4 Volatile Distribution

The volatiles CO_2 and H_2O have been ignored in the above discussion. However, their inclusion would not alter any of the above conclusions, for the volatiles, due to their high concentrations in the fluid phase, are considered to be K-components and will not define extra phases. Extensive loss of both CO_2 and H_2O must occur in the formation of the calc-silicate

phases. However, little evidence remains of their distribution during metamorphism. Further investigation of the anorthite alteration may lead to a greater knowledge of the volatile transfer. If the anorthite alteration involves the introduction of CO_2 (as expected from its proximity to the marble boundary, Section 5.4) then the movement of volatiles across the original contact appears to have been dominated by the diffusion of CO_2 into the pelite. This influx of CO_2 may cause further H_2O to be lost from the rock. Water escaping from the rock during metamorphism may also remove some $KO_{\frac{1}{2}}$ and FeO, as suggested in Section 5.7.

5.9.5 Felsic Layer

This layer is designated by an accumulation of K-feldspar and sphene, sometimes only as thin rims along the pelite edge of the original boundary. Hence, it appears to represent a concentration of the non-diffusing components, $KO_{\frac{1}{2}}$ and TiO_2. Therefore, its formation may result from a passive concentration of these components, in response to an extensive loss of the diffusing components. This is possibly associated with a physical movement of the original boundary (an extremely small distance) toward the pelite side, to compensate for the decrease in volume in the felsic layer. Such a process is discussed by Sanford (1980). Alternatively, if some movement of $KO_{\frac{1}{2}}$ and TiO_2 has been possible across the reaction band towards the marble, the felsic layer could represent an accumulation of these components derived from the conversion of the original pelite. Diffusion of $KO_{\frac{1}{2}}$ and TiO_2 into the original marble would have been quickly arrested by the inability of phases containing these components to form in equilibrium with the pore fluid.

5.9.6 Reaction Bands Involving the Garnet-rich Matrix

Garnet-rich Matrix

The garnet-rich matrix occupies a major proportion of the calcirudites, encompassing both pelitic and marble blocks, and is clearly not part of the pelite → marble reaction bands. However, with reference to the phase rule its simple mineralogy of predominantly garnet and minor clinopyroxene possibly suggests that diffusion has been important in its formation. From reactions occurring between the matrix and its included blocks (see below), diffusion of SiO_2, CaO, MgO and $AlO_{3/2}$ appears to have

occurred both into and out of the matrix.

Secondary phases occur interstitially amongst the garnet. These are dominated by coarse calcite and, to a lesser degree, quartz. Cu-Fe sulphides, mainly bornite and calcopyrite (Section 5.4), are also common, and prehnite and K-feldspar occur in minor amounts. The stability of calcite and quartz in preference to wollastonite suggests that these phases have crystallised below the peak of metamorphism. These phases are believed to represent the lower-temperature crystallisation of solutions present in the porous matrix. These solutions may have resulted from the formation of the high-grade silicates within the calcirudites, they may have been introduced into the rock either during or after metamorphism, or possibly they represent a combination of both processes.

Garnet-rich Matrix → Pelite Reaction Bands

The layer sequence in the pelitic material next to the matrix is identical to that next to the marble. Relative to the pelite, the matrix has acted as a source of calcium. The petrogenesis of this layering can be considered as similar to that for the marble → pelite reaction bands described above.

Garnet-rich Matrix → Marble Reaction Bands

These reaction bands are commonly represented by a rim of wollastonite within the original marble (Section 5.4). This seems to result from the simple diffusion of SiO_2 from the matrix into the marble, and the reciprocal loss of CaO into the matrix. With the lack of Al, wollastonite is the stable phase defined by the chemical potentials of SiO_2 and CaO (Fig. 5-5). Although both SiO_2 and CaO are diffusing components, the formation of wollastonite allows only one to be a K-component, and hence the phase rule is satisfied:

$$F(2) = C(2) - P(1) + (2) - m(1)$$

A second type of wollastonite layer has been recognised between the matrix and marble. These are commonly quite wide (1-2 cm) and consist of wollastonite, garnet, and lesser clinopyroxene (Section 5.4). These layers require diffusion of SiO_2, $AlO_{3/2}$, and MgO into the marble, and CaO into the matrix. Formation of this type of layer is similar to the formation of the garnet + clinopyroxene layer in the marble → pelite reaction bands. However, the chemical potential of $AlO_{3/2}$ diffusing into the marble appears

to be lower, allowing both wollastonite and garnet to form together (Fig. 5-5). Only one component in the wollastonite + garnet + clinopyroxene layer can be considered as a K-component.

Discussion

Two distinct features distinguish the reaction bands involving the garnet-rich matrix from the pelite → marble reaction bands. These are firstly, the much greater width of the layers, and secondly, the presence of wollastonite. The wider layers seem to require more extensive diffusion of the components (higher fluxes) than occurs in the exchange of components between adjacent blocks of marble and pelite. This is believed to be related to 1) the relatively large volume of original matrix which has been converted to the simple garnet + clinopyroxene assemblage, compared to the small volumes of material affected in the marble → pelite reaction bands, and 2) the high proportion of pore fluid within the resulting garnet-rich matrix, which has allowed extensive diffusion to take place (Vidale, 1969).

The presence of wollastonite between the marble and matrix suggests that the chemical potential of $AlO_{3/2}$ relative to CaO and SiO_2 is lower than in the marble → pelite reaction bands. Therefore, it appears that available $AlO_{3/2}$ was readily used in the formation of garnet, and $AlO_{3/2}$ diffusion into the marble was limited relative to SiO_2.

5.10 FURTHER EXAMPLES OF REACTION BANDS

Several other examples of reaction bands occur at the Horse Arm Creek locality (Fig. 5-1) and two are briefly described here for comparison with the reaction bands outlined above.

5.10.1 Sample T77B

This example shows a well developed reaction band between blocks of marble and lithic greywacke:

marble
wollastonite
garnet
garnet + clinopyroxene
felsic (K-feldspar + sphene ± clinopyroxene ± plagioclase)
clinopyroxene + feldspar + sphene
hornblende + feldspar + sphene
greywacke

As in the marble → pelite reaction bands of sample locality 371, the felsic : garnet + clinopyroxene layer boundary is marked by a sharp change in grainsize, and a thin concentration of sphene is noted on the greywacke side of the boundary. The width of this reaction band is much wider than that of the marble → pelite reaction bands, ranging from 0.5 to 1.0 cm. This may be related to greater permeability of the greywacke compared to the pelite. The sequence of layers is very similar to that in the marble → pelite reaction bands, except for the presence of a wollastonite layer and a hornblende-bearing layer. The wollastonite layer is readily explained by a greater flux of SiO_2 relative to $AlO_{3/2}$ in the marble → greywacke reaction band (the garnet layer ends by intersection of Y-Z rather than X-Y in Fig. 5-5). The higher SiO_2 flux reflects the higher initial SiO_2 content of the greywacke compared to the pelite. The formation of the hornblene-bearing layer is probably also related to the higher chemical potential of SiO_2, with hornblende having a higher SiO_2/CaO ratio than clinopyroxene.

5.10.2 Sample T73A

In this sample a reaction band has formed between interlayered carbonate and siliceous sediments:

marble
wollastonite
garnet
garnet + clinopyroxene
clinopyroxene + feldspar + sphene
clinopyroxene + feldspar + sphene + quartz

Extensive diffusion appears to have taken place, with the wollastonite layer being typically over 5 mm wide (having replaced most of the carbonate), and the siliceous unit (over 2 cm wide) has been totally replaced (in this sample) by clinopyroxene-bearing layers. The abundant formation of wollastonite is again associated with a high SiO_2 content in the original non-carbonate lithology, as exemplified by the presence of quartz in the layer furthest from the marble.

5.10.3 Discussion

The examples described above, and many others from the South Kootingal and Seven Mile Creek localities (Chapter Four) contain reaction bands which are similar to, and can be interpreted in the same manner as, those described in the earlier parts of this chapter. Probe analyses on

phases within these additional examples show that major differences in composition occur between phases analysed within the reaction bands of different localities. However, as noted in Section 5.5, little variation in mineral chemistry occurs across a single reaction band. This is summarized for samples T77B and T73A of this section, and the group of samples studied in previous sections from sample locality 371; the paired figures represent the range across a reaction band (or bands):

	T73A	T77B	371
$Mg/Mg+Fe^{2+}$ ratio of clinopyroxene	0.49-0.60	0.71-0.76	0.77-0.91
$Al/Al+Fe^{3+}$ ratio of garnet	0.27-0.28	0.41-0.63	0.65-0.85

These analyses appear to reflect variations in Fe content in the non-carbonate portion of the original rocks. Apparently, phase compositions within the reaction bands are more obviously determined by host-rock composition than by properties associated with the diffusion of components through a fluid medium (i.e. diffusion coefficients and solubilities).

The range of mineral compositions within these rocks has allowed differences in the optical properties of the phases to be related to variations in mineral chemistry. With decreasing Mg/Mg+Fe values, the clinopyroxenes have a darker green colour and more distinct pleochroism (also noted by Heinrich, 1965). Increasing substitution of Fe^{3+} and Al^{3+} in the clinopyroxenes also occurs with decreasing Mg/Mg+Fe. Similarly, garnet grains become darker in colour with decreasing Al/Al+Fe ratios. Grossular-rich garnets are typically colourless (or almost so), whereas andradite-rich garnets usually possess a darker orange-brown colour. Grossular-rich garnets are also typically birefringent and show well developed optical zoning. However, the garnets become isotropic with decreasing Al/Al+Fe. Almandine substitution in the garnets also increases slightly with decreasing Al/Al+Fe.

5.11 LARGER-SCALE DIFFUSION

An example of larger-scale diffusion has been studied between the western limestone horizon and the underlying lithic greywacke of the Horse Arm Creek locality (at sample locality T82, Fig. 5-1). The grey-black colour of the greywacke is altered to a greenish colour within ½-1m

of the limestone. T82C and T82A are samples of "unaltered" and "altered" greywacke respectively. The "unaltered" greywacke consists of relict crystal fragments of quartz and feldspar in a fine-grained groundmass of biotite, quartz, feldspar and Fe oxides. The "altered" greywacke (T82A) has an identical texture to that of T82C, but the fine-grained groundmass consists of clinopyroxene (giving the rock its greenish colour), quartz, feldspar and sphene. Analyses of the ferromagnesian phases and sphene in these samples are shown in Table 5.7.

Whole-rock analyses of both samples are also presented in Table 5.8. The most obvious difference is the significant increase in CaO from T82C to T82A. CO_2 is present in T82A, whereas it is absent in the "unaltered" greywacke. If the analysis of T82A is adjusted for the increase in CaO (and minor CO_2), so that its CaO content is reduced to that of T82C (i.e. 1.87%), then the two analyses become very similar in most of the other major components. This suggests that the alteration of the greywacke has primarily involved the introduction of $CaCO_3$ from the adjacent limestone. However, two important effects are noticed. Firstly, the increase in CaO has caused a marked decrease in K_2O, even though Na_2O has remained virtually unchanged. Secondly, although total iron has remained virtually the same, there has been a major decrease in the Fe_2O_3/FeO ratio of the Ca-enriched greywacke compared to the greywacke analysis of T82C.

Mineralogically, the introduction of CaO has caused the biotite + Fe oxide assemblage to be replaced by clinopyroxene + sphene. This change could be represented by the reaction describing the breakdown of biotite + calcite to clinopyroxene + K-feldspar (Thompson, 1975a). The clinopyroxene in sample T82A is far richer in Fe (Mg/Mg+Fe = 0.303) than the corresponding biotite (Mg/Mg+Fe = 0.620) in sample T82C (Table 5.7). Therefore, Fe originally present in opaque oxides seems to have been used in the formation of clinopyroxene, requiring change in oxidation state of the Fe. This is consistent with a comparison of the whole-rock compositions in Table 5.8. However, no increase in K-feldspar accompanies the formation of clinopyroxene, as expected from the above reaction. Hence, K_2O derived from the breakdown of biotite appears to be lost from the rock, as indicated by the decrease in K_2O in T82A relative to T82C (Table 5.8). Excess Al_2O_3, derived from the biotite breakdown, apparently combines with CaO to form a more-calcic plagioclase. Loss of K_2O from the CaO-enriched sediment was also recognised in the small-scale reaction bands (Section 5.7).

TABLE 5.7. Representative microprobe analyses from samples T82C and T82A

	T82C	T82A	
	BIOTITE	CLINOPYROXENE	SPHENE
SiO_2	36.58	49.97	30.66
TiO_2	2.04	-	36.93
Al_2O_3	19.43	0.39	1.50
Fe_2O_3		*0.61	-
FeO	14.37	20.50	0.87
MnO	-	0.19	-
MgO	13.17	4.99	-
CaO	-	23.96	29.60
Na_2O	0.16	-	-
K_2O	10.06	-	-
TOTAL	95.81	100.61	99.56
Structural formulae			
No. of oxygens	22	6	10
Si	5.408	1.976	2.018
Al^{IV}	2.592	0.018	
Al^{VI}	0.796	-	0.116
Ti	0.227	-	1.828
Fe^{3+}		0.018	-
Fe^{2+}	1.777	0.678	0.048
Mn	-	0.006	-
Mg	2.902	0.294	-
Ca	-	1.015	2.087
Na	0.046	-	-
K	1.898	-	-
Total cations	15.646	4.005	6.097
$Mg/Mg+Fe^{2+}$	0.620	0.303	

* Fe_2O_3 calculated by method of Papike *et al.* (1974).

TABLE 5.8. Comparative chemical analyses of samples T82C and T82A

	"UNALTERED" GREYWACKE T82C	"ALTERED" GREYWACKE T82A	ADJUSTED ANALYSIS OF T82A
SiO_2	63.44	53.96	62.35
TiO_2	0.65	0.75	0.87
Al_2O_3	15.57	14.40	16.64
Fe_2O_3	5.32	1.35	1.56
FeO	3.34	7.79	9.00
MnO	0.04	0.13	0.15
MgO	2.59	2.00	2.31
CaO	1.87	15.00	1.87
Na_2O	3.75	3.16	3.65
K_2O	2.11	0.25	0.29
P_2O_5	0.10	0.11	0.13
H_2O^+	1.05	0.40	0.46
H_2O^-	0.10	0.32	0.37
CO_2	-	0.31	-
Insoluble	0.07	0.07	
Sr	204	362	
Rb	39	-	
Y	19	20	
Zr	64	43	
Nb	5	3	

The adjusted analysis of T82A is calculated by reducing the CaO and CO_2 values of T82A to those of T82C, and normalising to 100%. Analyses by G.I. Kolocsai. All analyses by wet chemistry (SiO_2 by difference).

This could be related to the high solubility of K in aqueous solutions (Vidale, 1969) which are lost from the rocks during metamorphism. The loss of H_2O may be enhanced by the influx of CO_2 (a possibility suggested in Section 5.9.4). Based on probe data and the above discussion, a possible reaction for the CaO alteration of the greywacke is given as:

1.00 Biotite + 2.61 Hematite + 18.48 Quartz + 12.22 Calcite
→ 10.00 Clinopyroxene + 1.68 Anorthite + 0.53 Sphene + 2.00 H_2O + 12.22 CO_2 + K_2O

REACTANTS

Biotite $K_2Al_{.80}Ti_{.23}Fe_{1.78}Mg_{2.90}Si_{5.4}Al_{2.6}O_{20}(OH)_4$

PRODUCTS

Clinopyroxene $Ca_{1.00}Fe_{.70}Mg_{.29}Si_2O_6$

Sphene $Ca_{1.00}Ti_{0.43}Al_{0.07}Si_1O_5$

5.12 SUMMARY AND CONCLUSIONS

Several examples of small-scale reaction bands (typically less than 2 cm wide) have been studied within a calcirudite containing blocks of pelite and marble. The samples studied in detail were collected from the one locality, and are believed to have been contact metamorphosed at temperatures of between 610 and 650°C, and pressures below 2 kb. Reaction bands have developed between the original matrix of the calcirudite and the included blocks, as well as between the individual blocks. The characteristic sequence of layers between the marble and pelite blocks is believed to be

marble
garnet
garnet + clinopyroxene
felsic (K-feldspar + sphene ± clinopyroxene ± plagioclase)
clinopyroxene + feldspar + sphene
biotite + feldspar + sphene
biotite + feldspar unit
pelite

However, unaltered pelite was not observed in the reaction bands studied. The original contact between marble and pelite is believed to be represented by the boundary between the garnet + clinopyroxene and felsic layers. This boundary is characterised texturally by a sharp

change in grainsize, and mineralogically by the lack of K_2O- and TiO_2-bearing phases on the marble side of the boundary. The layer sequence developed between the pelite blocks and matrix is similar to that in the marble → pelite reaction bands:

garnet-rich matrix
garnet + clinopyroxene
felsic
clinopyroxene + feldspar + sphene
biotite + feldspar + sphene
biotite + feldspar unit

At contacts between matrix and marble blocks, either a monominerallic wollastonite layer, or a wollastonite + garnet + clinopyroxene layer is developed within the original marble. Layering associated with the garnet-rich matrix is typically much wider than that in the marble → pelite reaction bands.

Study of the mineral chemistry across the reaction bands, especially clinopyroxene and garnet, shows that variations between grains are no greater than those within grains, and no systematic changes were detected across the reaction bands. The compositional similarity between clinopyroxenes from layers formed on either side of the original boundary suggests that the ratio of MgO and FeO diffusing into the marble is related to the MgO/MgO+FeO ratio of the non-carbonate rock. This compositional control of host rock on the phases being formed during diffusion has been recognised for a range of non-carbonate rock types.

Chemical variations across the reaction bands show sharp changes in composition at layer boundaries. Notably, CaO shows a stepwise decrease across the reaction band away from the marble, whereas Al_2O_3 and MgO (+FeO) decrease away from the pelite, but increase in the garnet and garnet + clinopyroxene layers respectively. SiO_2 content appears to remain relatively constant across the reaction bands. Plots of layer compositions on ACF diagrams show a general trend toward the CaO corner. However, a continuous path involving three-phase assemblages separated by two-phase boundaries does not exist, because diffusion involves continuous changes in the chemical potentials of the diffusing components, rather than their molar amounts. Major deviations are present from the general trend toward the CaO corner, because diffusion of $AlO_{3/2}$, MgO and SiO_2 has also occurred, and uniform ratios between these components are not

maintained during diffusion.

Mass balance calculations on a marble → pelite reaction band show excellent balance for MgO and Al_2O_3. The major imbalances occur in SiO_2 and, to a lesser degree, CaO. These calculations suggest that a decrease in volume has occurred on the marble side of the original boundary. However, a major decrease in volume of the non-carbonate side of the reaction band may not be necessary if the original pelite contained quartz, and if the biotite + feldspar unit represents pelite enriched in CaO. The decrease in volume of the marble is consistent with the loss of CO_2, and it is tentatively proposed that CO_2 has diffused into the original pelite (resulting in the alteration of anorthite). This influx of CO_2 could enhance the loss of H_2O from the rock during metamorphism. This escaping H_2O may also remove dissolved $KO_{\frac{1}{2}}$ and FeO, as possibly required by the mass balance calculations.

The reaction bands are believed to have developed by the mass transfer of components between chemically incompatible rock types. A model has been suggested whereby the components diffuse through a pore solution in response to chemical potential gradients in the solution (concentration gradients). These gradients are maintained by removal of material from solution, as solid phases in equilibrium with the fluid are formed. Diffusion proceeds so as to reduce these gradients and, with time, discontinuities are eliminated and the chemical potentials of the diffusing components will vary monotonically and continuously across the reaction band. Local equilibrium is considered to be achieved at each point across the reaction band. The solid phases in local equilibrium with the diffusing components of the pore fluid can be expressed on chemical potential diagrams. The layers develop across the reaction band as new phases become stable in response to the continuously changing chemical potentials of the diffusing components and the presence or absence of non-diffusing components. The layers represent distinct changes in mineral assemblage, and the layer boundaries mark sharp discontinuities in bulk rock composition.

The number of phases in the layers is typically less than the number of components. The relationship between the number of phases and components can be expressed by the phase rule in terms of J- and K-components. Non-diffusing components have their chemical potentials internally controlled

by the original composition of the rock type, and are termed J-components. Chemical potentials of the diffusing components vary across the zones and will have their chemical potentials externally controlled in relation to points of local equilibrium. However, not all diffusing components can be considered to be K-components, because each phase in equilibrium with a number of diffusing components in the pore fluid reduces by one the number of these diffusing components that can be chosen independently. However, it is not appropriate to specify which of the diffusing components are K-components and which are J-components, for this would imply that differences exist in their behaviour during diffusion, which is not correct. Therefore, attempts to recognise J- and K-components in the reaction bands are of little use in predicting layer assemblages. An understanding of the development of layers within the reaction bands requires identification of the diffusing and non-diffusing components, and a knowledge of how solid phases in equilibrium with the pore fluid vary with changes in the chemical potentials of the diffusing components. Recognition of the number of J- and K-components for a given assemblage follows from a knowledge of the number and identity of phases in equilibrium with the diffusing components.

The relative movement of components can be discussed in terms of flux (amount moved) and distance moved. Because the diffusion coefficients of the various components in a pore solution are believed to be similar at the temperatures and pressures of metamorphism, flux is related primarily to chemical potential gradients in the pore fluid. Although the relative solubilities of the components are likely to affect their chemical gradients, in this study flux appears to be directly related to compositional differences in the components between the two initially chemically incompatible rock types. The relative distances to which the components have diffused across the original boundary appear to simply depend on the flux of each component and the rate at which it is used by the solid phases forming in equilibrium with the pore fluid.

Reaction bands involving the garnet-rich matrix are typically wider than the marble → pelite reaction bands, apparently reflecting the higher fluxes of the components diffusing out the garnet-rich matrix, compared to the small exchange of components possible between blocks of marble and pelite. These higher fluxes are believed to be related to the extensive interaction of pelitic and calcareous material in the matrix,

and the high proportion of pore fluid amongst the matrix assemblage. The garnet-rich matrix → marble reaction bands are characterised by a wollastonite layer. The presence of wollastonite reflects a lower $\mu AlO_{3/2}/\mu SiO_2$ ratio in the diffusing components relative to the marble → pelite reaction bands.

Further examples of reaction bands from the inner aureole of the Inlet Monzonite show a similar sequence of layers to those in the marble → pelite reaction band. Differences that do occur (commonly the formation of a wollastonite layer) are believed to reflect variations in the original composition of the non-carbonate rock type. An example of larger-scale diffusion is illustrated by the alteration of a greywacke adjacent to a limestone unit. Alteration of the greywacke appears to have mainly involved the introduction of CaO and CO_2 from the limestone, a loss of K_2O, and a change in the oxidation state of Fe.